12
10/28/91 Qm (1)

PNL-7792
UC-802

Sensitivity and Uncertainty Analyses of Unsaturated Flow Travel Time in The CHnz Unit of Yucca Mountain, Nevada

W. E. Nichols
M. D. Freshley

October 1991

Prepared for the U.S. Department of Energy
under Contract DE-AC06-76RLO 1830

Pacific Northwest Laboratory
Operated for the U.S. Department of Energy
by Battelle Memorial Institute

Battelle

PNL-7792

DISCLAIMER

PACIFIC NORTHWEST LABORATORY
operated by
BATTELLE MEMORIAL INSTITUTE
for the
UNITED STATES DEPARTMENT OF ENERGY
under Contract DE-AC06-76RLO 1830

Printed in the United States of America

Available to DOE and DOE contractors from the Office of Scientific and Technical Information, P.O. Box 62, Oak Ridge, TN 37831; prices available from (615) 576-8401. FTS 626-8401.

Available to the public from the National Technical Information Service, U.S. Department of Commerce, 5285 Port Royal Rd., Springfield, VA 22161.

PNL--7792

DE92 001852

SENSITIVITY AND UNCERTAINTY ANALYSES OF UNSATURATED FLOW TRAVEL TIME IN THE CHnz UNIT OF YUCCA MOUNTAIN, NEVADA

W. E. Nichols
M. D. Freshley

October 1991

Prepared for
the U. S. Department of Energy
under Contract DE-AC06-76RLO 1830

Pacific Northwest Laboratory
Richland, Washington 99352

EXECUTIVE SUMMARY

This report documents the results of sensitivity and uncertainty analyses conducted to improve understanding of unsaturated zone ground-water travel time distribution at Yucca Mountain, Nevada. The U.S. Department of Energy (DOE) is currently performing detailed studies at Yucca Mountain to determine its suitability as a host for a geologic repository for the containment of high-level nuclear wastes. As part of these studies, DOE is conducting a series of Performance Assessment Calculational Exercises, referred to as the PACE problems. The work documented in this report represents a part of the PACE-90 problems that addresses the effects of natural barriers of the site that will stop or impede the long-term movement of radionuclides from the potential repository to the accessible environment. In particular, analyses described in this report were designed to investigate the sensitivity of the ground-water travel time distribution to different input parameters and the impact of uncertainty associated with those input parameters. Five input parameters were investigated in this study: recharge rate, saturated hydraulic conductivity, matrix porosity, and two curve-fitting parameters used for the van Genuchten relations to quantify the unsaturated moisture-retention and hydraulic characteristics of the matrix.

Simulations were performed with a numerical code to solve the governing equations of flow under unsaturated conditions. A numerical algorithm was used to calculate travel time based on the solution of the governing equations. The code used was PORFLO-3©(a), a mathematical model for fluid flow, heat, and mass transport in variably saturated geologic media. For uncertainty analyses, a Monte Carlo version of PORFLO-3© ("PORMC") was used. All simulations were for steady-state, one-dimensional models of the Calico Hills nonwelded zeolitic (CHnz) hydrostratigraphic unit at Yucca Mountain. The simplicity of this preliminary work permitted development of verifiable procedures and computer codes that could be expanded later to include more complex descriptions of travel time distribution at Yucca Mountain.

A sensitivity study was conducted with sensitivity coefficients computed from the results of a collection of PORFLO-3© deterministic simulations of water flow in the CHnz unit. The results identified matrix porosity as the parameter to which unsaturated zone ground-water travel time is most sensitive, followed by recharge rate. The response of travel time was relatively insensitive to the other three parameters (saturated hydraulic conductivity and the two van Genuchten parameters α and n).

An uncertainty study was conducted based on Monte Carlo stochastic simulations of travel time through the CHnz unit model. A series of single-variable stochastic simulations illustrated the response of the travel-time distribution to uncertainty in each of the five input parameters. A simultaneous multi-variable stochastic simulation demonstrated the effect on the travel time distribution caused by uncertainty

(a) PORFLO-3© is copyrighted by Computational and Analytic Research, Incorporated subject to the Limited Government License.

in all five input parameters. The results of these simulations showed that uncertainty in the recharge rate is responsible for most of the variation in the travel time distribution. Matrix porosity was the next most significant variable, while the remaining three were much less important.

The results of the sensitivity study and the uncertainty study were contrasted with Yucca Mountain investigations performed by other researchers. With respect to the differences in methods and assumptions, the results and conclusions from this work agree with those of similar investigations.

Combining the results of the sensitivity and uncertainty analyses leads to the conclusion that the two variables that are most important to quantify to reduce variability in travel time estimates are the recharge rate and the matrix porosity. Although the saturated hydraulic conductivity and the van Genuchten parameters are important to the flow solution, the travel time calculation is relatively insensitive to variations in these parameters.

CONTENTS

FIGURES

TABLES

1.0 INTRODUCTION

The U.S. Department of Energy (DOE) Office of Civilian Radioactive Waste Management is currently performing detailed studies at Yucca Mountain, Nevada to determine its suitability as a host for a geologic repository for the containment of high-level nuclear wastes. Yucca Mountain is within the physiographic Basin and Range Province, which is characterized by north-south trending mountain ranges and intervening valleys. Yucca Mountain (Figure 1.1) is a prominent group of north-trending fault block ridges. The elevation of northern Yucca Mountain is approximately 1500 m and the ridge is approximately 300 m above the valley floor. Yucca Mountain is comprised of both welded and nonwelded volcanic tuffs that dip 5 to 10 degrees to the east (Montazer and Wilson 1984). The densely welded tuffs are typically highly fractured with low saturated matrix hydraulic conductivities (Peters and Klavetter 1988). The nonwelded tuffs that are vitric have few fractures and relatively high saturated matrix hydraulic conductivities, while the zeolitic nonwelded tuffs are characterized by low matrix hydraulic conductivities. Major geologic features intersecting the mountain include the Solitario Canyon Fault and the Ghost Dance Fault.

The unsaturated zone at Yucca Mountain is characterized by a low recharge rate. A conceptual model of flow through Yucca Mountain (Montazer and Wilson 1984) is presented in Figure 1.2. In the current conceptualization of flow through the mountain, a small fraction of the annual precipitation at the mountain migrates as recharge downward through the tuff units toward the water table. Some water movement within Yucca Mountain occurs as water vapor which can move in an upward direction. Most of the liquid water most likely moves predominantly in a vertical downward direction. Geologic, hydrologic, and geochemical features of the site form natural barriers for movement of radionuclides from a prospective repository. A measure of the performance of natural barrier systems is the travel time for water and contaminants to move from a specific location to another, usually from a point of release for contaminants to the accessible environment where exposures to human populations can occur. The travel time performance measure is specifically called out in the regulations (10 CFR 60.113; 10 CFR 960.5-2-1).

As part of the studies at Yucca Mountain, the DOE is conducting a series of Performance Assessment Calculational Exercises, referred to as the PACE problems. The PACE problems are designed to provide DOE with an opportunity to assess the capabilities of current performance assessment codes and to perform sensitivity studies. The Performance Assessment Scientific Support (PASS) Program at Pacific Northwest Laboratory (PNL)[a] participated in the PACE-90 problems, which are the set of problems being addressed during FY 1990. A part of the PACE-90 problems addresses the effects of natural barriers, which consist of geologic, hydrologic, and geochemical features of the site that will stop or

(a) Pacific Northwest Laboratory is operated by Battelle Memorial Institute for the U.S. Department of Energy under Contract DE-AC06-76RLO 1830.

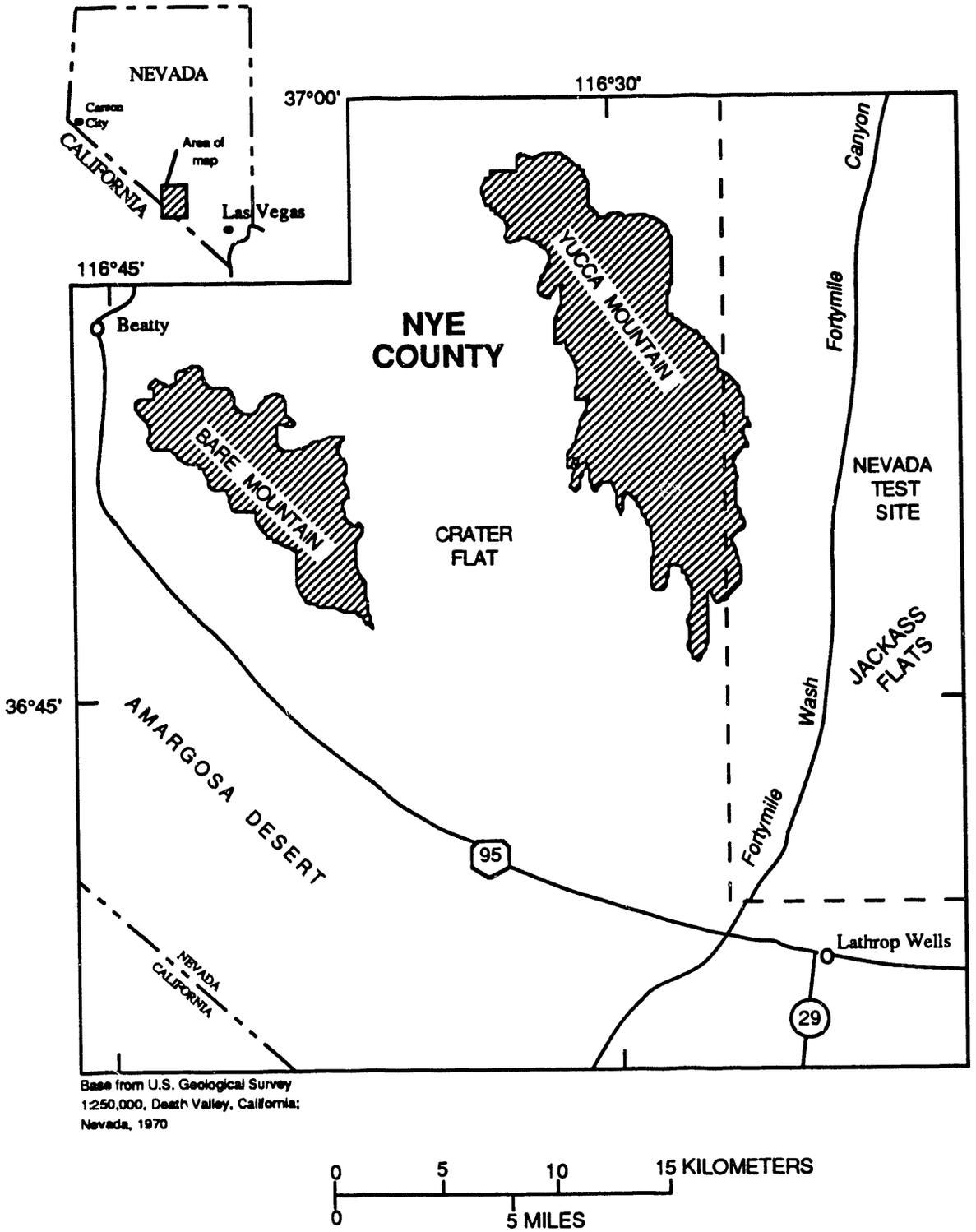

FIGURE 1.1. Physiographic Features of Yucca Mountain and Surrounding Region (Modified from Montazer and Wilson 1984)

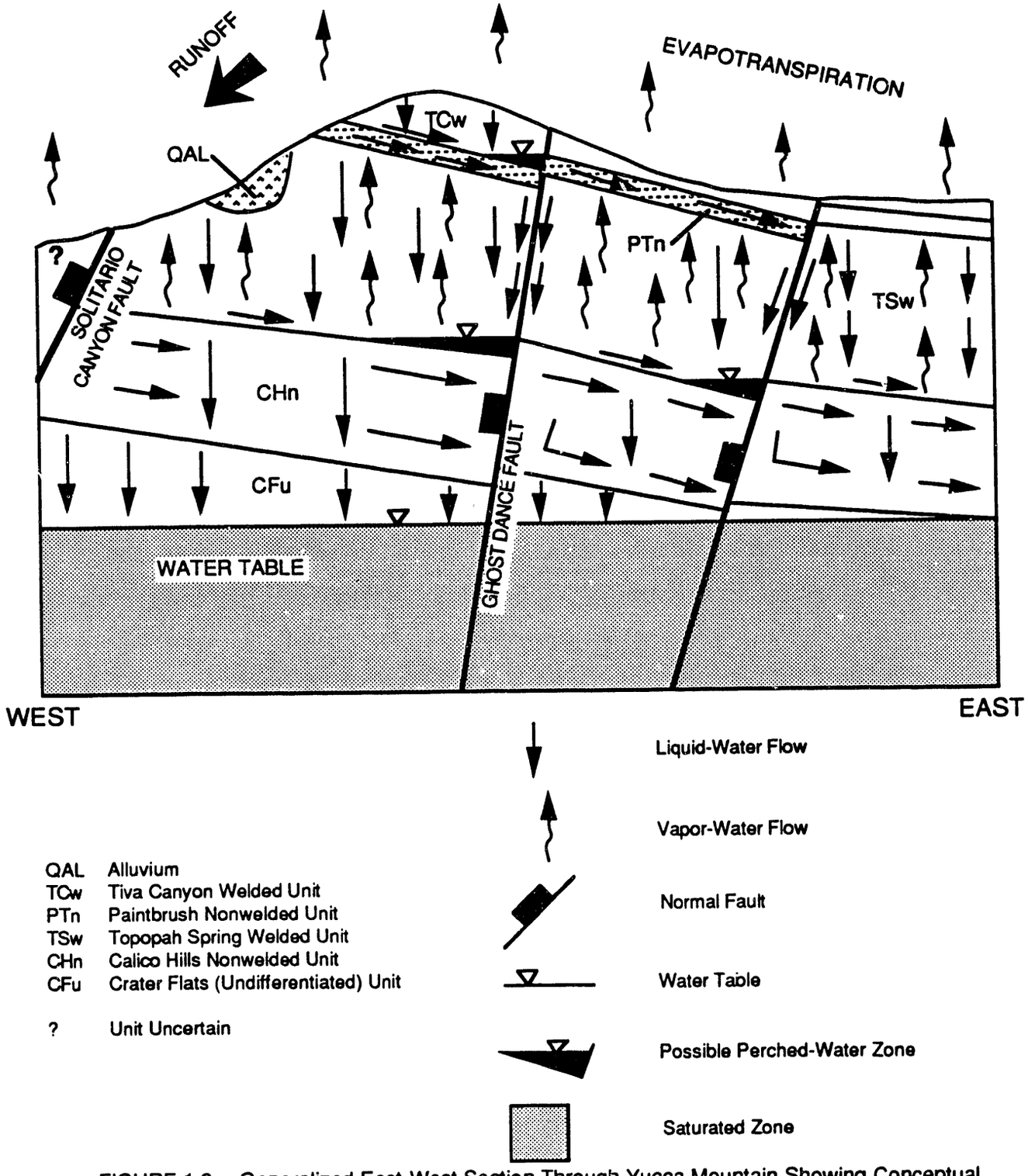

FIGURE 1.2. Generalized East-West Section Through Yucca Mountain Showing Conceptual Moisture-Flow System Under Natural Conditions (modified from Montazer and Wilson 1984)

impede the long-term movement of radionuclides from the potential repository to the accessible environment.

The PACE problem set for the natural barrier system includes cases that address the hydrologic conditions within the mountain prior to proposed emplacement of waste, post-emplacement hydrology, formation of perched water, sensitivity of ground-water travel times, fracture-matrix interactions, and upgrading of computer codes. This report includes descriptions of analyses devoted to the investigation of ground-water travel time at Yucca Mountain. Both sensitivity of ground-water travel time to variation of input parameters and uncertainty in the ground-water travel time distribution due to uncertainty in input parameters are discussed.

Descriptions of the other natural barrier problems that were addressed by staff in the PASS Program are presented in the following reports. Results of the perched water table analysis are described by Freshley and Aimo (1990)[a]. The results of the fracture-matrix investigation is provided by Smoot and Wurstner (1990)[b]. A description of the upgrades to the PORFLO-3© computer code, with respect to both the mathematical formulations and the input data, is presented in White (1990)[c].

(a) Freshley, M. D. and N. J. Aimo. 1990. Evaluation of Conditions for Perched Water Formation Within Yucca Mountain, Nevada, Draft Letter Report for U.S. Department of Energy prepared by Pacific Northwest Laboratory, Richland, Washington.

(b) Smoot, J. L., and S. K. Wurstner. 1990. Flow Through Variable Aperture Fractures: FY 1990 Summary Report on the Sensitivity of Fracture-Matrix Interactions. Draft Letter Report for U.S. Department of Energy prepared by Pacific Northwest Laboratory, Richland, Washington.

(c) White, M. D. 1990. MSTS: A Simulator for Multiphase Subsurface Transport. Draft Letter Report for U.S. Department of Energy prepared by Pacific Northwest Laboratory, Richland, Washington.

2.0 DISCUSSION OF TRAVEL TIME

A discussion of any technical subject requires definition of terminology used to describe complex ideas and phenomena. These definitions can vary between researchers, as is the case with the term "travel time" used in this report. In the description of the PACE-90 problem set and in the documents supporting the Yucca Mountain investigation (DOE 1986, DOE 1988), the term "ground-water travel time" is used to describe travel time in the unsaturated zone at Yucca Mountain. However, because the term "ground water" is often interpreted to describe water in the fully saturated zone, the term unsaturated zone travel time (UZTT) is used in this report to emphasize that we are concerned with water movement in the unsaturated zone.

Travel time is generally defined as the average length of time for water or miscible contaminants to move from point A to point B along a particular flow path in either unsaturated or saturated flow regimes. Another definition for travel time at an outflow boundary is arrival time, in reference to the time at which water or a contaminant reaches the boundary.

Travel time may be estimated by a number of different methods. Estimates of travel time can be based on long-term observations of tracers that are either natural or were introduced to the environment by humans, local observations of contaminant or tracer movement and extrapolation of the local velocities, or by hand calculation or application of numerical models. It may be possible at Yucca Mountain to estimate travel times by observation of environmental tracers such as chlorine-36 and carbon-14 or by introduction of other tracers on a local scale. However, the most common method of estimating travel times through Yucca Mountain is by application of numerical models.

Distributions of travel time reflect both variations in flow paths and uncertainties in the parameters used to estimate travel time, if calculations are performed. In a multidimensional flow field, variations between water flow paths tend to spread travel times around the average time. The dimension of hydrodynamic dispersion along each flow path is added for contaminant transport which results in further spreading of travel times. In addition, with contaminant discharge at an outflow boundary, there is a spatial distribution of contaminants along with the distribution in time (Nelson 1978). Contaminant distributions at outflow boundaries may be referred to as arrival distributions. In addition, if calculations are performed to estimate the travel times, uncertainties in the input parameters will result in uncertainties in the calculated travel times. These uncertainties in both input and output parameters are expressed as distributions.

One guideline prescribed by the DOE for siting a high-level nuclear waste repository is the 1000-year minimum ground-water travel time calculated for a site prior to waste emplacement (DOE 1984). The time is to be evaluated for any potential path of likely radionuclide travel from the disturbed zone near the potential repository to the accessible environment. The DOE guidelines call for disqualification of a

site if the expected ground-water travel time along any path of likely significant radionuclide travel is less than 1000 years. To establish credibility and to demonstrate compliance with regulatory standards, it will be necessary determine the uncertainty in the travel time estimates, expressed as distributions of travel time.

In this report, the expression "travel time computation" refers to a calculation based on the mean pore-water velocity in the domain of interest. In examining a travel time distribution, we refer to the distribution of travel times that results from variation of an input variable or variables used to calculate travel time.

3.0 CALCULATION OF UNSATURATED ZONE TRAVEL TIME

Assessment of the post-closure performance of a potential high-level nuclear waste repository at Yucca Mountain, Nevada requires calculation of water travel time in the geologic media, which in turn requires detailed knowledge of the physical characteristics of the media. A large effort has been conducted to document the physical properties of the geologic units that comprise Yucca Mountain. However, sampling these properties is difficult and expensive. Even more restricting is the fact that these properties are subject to varying degrees of spatial and sampling variability. At present, the physical parameters required to model the hydrologic processes of Yucca Mountain are not characterized to the extent required for licensing a high-level nuclear waste repository.

Numerical modeling of system performance with the preliminary values available for the physical properties provides useful information. In particular, this kind of modeling

- provides preliminary estimates of the time required for radionuclides to be transported through the unsaturated zone
- develops understanding of the distribution of water travel times in Yucca Mountain
- identifies the most important hydrologic characteristics in terms of their effect on water travel time.

Preliminary estimates of travel time can be used to address the issues of site suitability to determine if characterization should proceed. Preliminary estimates of travel time also help to "bracket" times of arrival for transport of non-attenuated contaminants. Study of the distribution of travel times in Yucca Mountain improves understanding of the dependence of water transport rates on key input parameters for describing unsaturated flow in numerical models. Finally, knowledge of the relative importance of key input parameters can help focus data collection efforts on characterization of parameters that most influence water movement, and hence, contaminant transport.

This study is preliminary, reflecting use of existing data for investigation of the distribution of travel times for water in the unsaturated zone of Yucca Mountain. The first steps in this investigation involve study of one-dimensional flow within the matrix of a single hydrostratigraphic unit (the Calico Hills unit). Future work could expand from this base to multiple-layer, multiple-dimension unsaturated flow through fractured tuff to provide more useful, detailed travel time information.

Flow through partially saturated fractures was not considered as part of this study because its preliminary nature. Neglecting fracture flow is valid for this investigation because the Calico Hills nonwelded unit is expected to contain fewer fractures than the welded tuff units present at Yucca Mountain. A separate investigation of matrix-fracture effects is reported in Smoot (1990).

This chapter is divided into two sections. Section 3.1 reviews the general equations solved by the variably saturated flow codes used in this study. Section 3.2 presents the travel time numerical algorithm that uses information generated by solution of the general flow equation to compute water travel time.

3.1 GOVERNING EQUATIONS OF FLOW

Calculation of travel time for water in porous media is based on the fundamental equations for quantifying flow behavior in the media. The governing equations solved by the PORFLO-3 computer code and its derivative PORMC (Runchal and Sagar 1989, Sagar and Runchal 1990) are presented because the travel time algorithm applied (presented in Section 3.2) is based on their solution. The equation for conservation of a slightly compressible fluid mass in nondeforming media is expressed as

$$\partial(\theta\rho) + \vec{\nabla}\cdot(\rho\vec{V}) - M = 0 \tag{3.1}$$

where ∂ = partial derivative

θ = volumetric moisture content ($m^3\ m^{-3}$)

ρ = fluid density ($kg\ m^{-3}$)

$\vec{\nabla}$ = vector differential operator

$\vec{V}$ = Darcy velocity vector ($m\ s^{-1}$)

M = fluid source/sink term ($kg\ s^{-1}$).

A complete list of notation is provided in Appendix A. The Darcy equation for nonisothermal flow is

$$\vec{V} = -\left(\frac{\mathbf{k}}{\mu}\right)\left(\vec{\nabla}p + \rho g\vec{\nabla}z\right) \tag{3.2}$$

where $\mathbf{k}$ = intrinsic permeability tensor (m^2)

μ = dynamic fluid viscosity ($m^{-1}\ s^{-1}$)

p = fluid pressure ($kg\ m^{-1}\ s^{-2}$)

g = acceleration due to gravity ($m\ s^{-2}$)

z = vertical direction in cartesian coordinate system, taken as positive upwards (m)

Equation (3.2) is substituted into Equation (3.1) to obtain the governing equation for single-phase fluid flow under nonisothermal conditions that is solved in the PORFLO-3 and PORMC codes:

$$S_S \partial_t H = \partial_x (R K_x \partial_x H) + \partial_y (R K_y \partial_y H) + \partial_z [R K_z (\partial_z H + B)] + \theta \beta_f R \partial_t T + M_V \quad (3.3)$$

where S_S = fluid storage term (m^{-1})

t = time (s)

H = hydraulic head with respect to reference fluid density (m)

x,y,z = directions in cartesian coordinate system (m)

R = ratio of fluid density

K = hydraulic conductivity in the direction denoted by x,y,z subscripts ($m\ s^{-1}$)

B = thermal buoyancy term

β_f = fluid compressibility ($m\ s^2\ kg^{-1}$)

T = temperature of fluid-containing geologic media (K)

M_V = fluid source term ($m^3\ s^{-1}$).

The fluid storage term (S_S) is defined by the following equations:

$$S_S = (\alpha_s + n_E\ \alpha_f)\ \rho g \quad (3.4a)$$

if $\theta = n_E$. If $\theta < n_E$,

$$S_S = \frac{\partial \theta}{\partial \psi} \quad (3.4b)$$

where α_s = compressibility of solid media ($m\ s^2\ kg^{-1}$)

n_E = effective or flow porosity ($m^3\ m^{-3}$)

α_f = compressibility of fluid ($m\ s^2\ kg^{-1}$)

ψ = soil moisture potential (= -P when $P < 0$).

The density ratio (R), the thermal buoyancy (B), and the hydraulic conductivity tensor (K) are computed using

$$R = \left(\frac{\rho}{\rho^*}\right) \tag{3.5}$$

$$B = R - 1 \tag{3.6}$$

$$K = \frac{\rho g k}{\mu} \tag{3.7}$$

where ρ^* is the fluid density at a reference temperature.

The above equations were written under the assumption that the principal directions of the hydraulic conductivity tensor coincide with the coordinate directions (x,y,z) such that only the diagonal terms of the tensor are nonzero (Runchal and Sagar 1989, Sagar and Runchal 1990).

Hydraulic head (H) and pressure head (P) are related by

$$H = P + (z - z^*) \tag{3.8}$$

where z^* is an arbitrary elevation datum, and the pressure head is defined by

$$P = \frac{p}{\rho g} \tag{3.9}$$

The pressure head (P) is larger than the atmospheric pressure head (and hence positive) for saturated flow, and is less than atmospheric pressure (and hence negative) for unsaturated flow. The volumetric moisture content (θ) is equal to the effective porosity (n_e) for saturated flow. The soil moisture potential (ψ) and intrinsic permeability (k) are functions of the volumetric moisture content (θ).

The governing equations are solved with an integrated finite-difference scheme by the PORFLO-3 and PORMC codes for a rectangular grid mesh. The solution of the general equation for fluid flow and the coupling equations leads to values of hydraulic head (H), relative saturation (θ^*), and fluid velocity (U, V, and W in the x, y, and z directions, respectively). This information is sufficient for computing travel time with the algorithm presented in the next section.

3.2 TRAVEL TIME COMPUTATIONAL ALGORITHM

The algorithm for computing travel time uses a particle-tracking, essentially Lagrangian, approach. A particle of water or contaminant is defined at a specified starting coordinate. The quantity desired is the time required for that particle to reach an ending coordinate or boundary (such as the water table or boundary of the problem domain). Travel time across each grid cell is calculated, beginning at the cell containing the starting coordinate. Travel time is based on the pore-water velocity, which is the fluid velocity divided by the effective porosity, or in the case of unsaturated flow, the effective saturation. The effective saturation ($n_E\theta^*$) is the water-filled pore space through which liquid flow occurs. For each grid cell the travel time is computed in each direction (x,y,z) using the directional velocities (U,V,W). The direction with the shortest travel time is used to identify the subsequent downstream cell. The process is repeated as the particle enters each new grid cell until the ending condition is met or the total simulation time is reached.

A verification exercise was undertaken to confirm the numerical accuracy of the travel time algorithm and to check its implementation in the PORFLO-3© and PORMC computer codes. The verification exercise and the results are presented in Appendix B. The final verification provided adequate confidence that the computer code implementing the algorithm was functioning properly.

In the following discussion, the travel time algorithm is presented for the x direction. The development is the same for the y and z directions. In any grid cell, the lower numerical value cell face coordinate value is denoted by X_i and the other cell face coordinate by X_{i+1}. The pore-water velocity at any point x within the grid cell is computed from

$$U_p = A_0 + A_1(x - X_i) \tag{3.10}$$

in which the flow coefficients A_0 and A_1 are expressed as

$$A_0 = \frac{U_i}{n_E\,\theta^*} \tag{3.11}$$

$$A_1 = \frac{U_{i+1} - U_i}{(X_{i+1} - X_i)(n_E\,\theta^*)} \tag{3.12}$$

where U_p = pore-water velocity in x-direction (m s^{-1})

U_i = x-direction Darcian velocity at cell face i (m s^{-1})

U_{i+1} = x-direction Darcian velocity at cell face i+1 (m s^{-1})

θ^* = relative saturation.

Note that the quantity $[U_{i+1} - U_i]$ represents the difference in velocities across the grid cell for the x direction. A_1 is zero for a steady-state case. Therefore, the pore-water velocity is equal to A_0 for steady-state conditions.

Equation (3.12) gives the pore-water velocity at any point as a function of position within the current cell. To compute the travel time, the equation

$$d_x t = \frac{dx}{U_p} \tag{3.13}$$

is integrated between time n-1 and time n, which yields

$$t^n - t^{n-1} = \frac{1}{A_1} \ln\left(\frac{A_0 + A_1(X^n - x_i)}{A_0 + A_1(X^{n-1} - x_i)}\right) \tag{3.14}$$

where ln is the natural logarithm function. Direct use of Equation (3.14) is limited because opportunity exists for division by zero and for computing the logarithm of zero. A_1 is zero when the velocity is constant across the cell in the x direction. In this event, Equations (3.10) and (3.13) reduce to

$$t^n - t^{n-1} = \frac{(X^n - X^{n-1})}{A_0} \tag{3.15}$$

Numerical solution of the governing equation for flow [Equation (3.3)] can produce small numerical differences in the velocity field across a cell. For example, in a one-dimensional steady-state problem, the term A_1 is zero by definition. Small numerical differences in U_i and U_{i+1} can lead to fictional nonzero values of A_1, which in turn produces a cumulative error in the travel time computation. To prevent this from occurring, Equation (3.15) is applied in preference to Equation (3.14) when the velocity of one side of the cell is much greater than the variation of velocity across the cell, i.e., when

$$A_0 >> A_1(X_{i+1} - X_i) \tag{3.16}$$

Observe that the numerator of the logarithm argument in Equation (3.14) is the velocity at the next location in the flow path (X^n) and the denominator is the velocity at the current location (X^{n-1}). These quantities are denoted by V^n and V^{n-1}, respectively. The terms V^n and V^{n-1} must have the same sign, otherwise the flow is convergent or divergent. In addition, if either V^n or V^{n-1} were equal to zero in one-dimensional, steady-state simulation the travel time would be infinite. If either of these conditions arises, the travel time computation is stopped and the error noted.

The travel time computation is performed in all three directions (x,y,z) for each grid cell. The next grid cell that a particle enters is determined by computing the travel time along each coordinate axis through the current cell. The downstream cell face normal to the axis for which the shortest travel time is computed is identified as the upstream cell face of the next cell.

For steady-state simulations, Equation (3.15) is used to determine the travel time through each grid cell of the flow path. For transient simulations, the governing equation is solved in time steps of size Δt. It is possible that the travel time across a given cell ($t^n - t^{n-1}$) is larger than Δt. In this event, the intermediate location within the cell is given as

$$X^n = X_i + \frac{\left\{A_0 + A_1\left(X^{n-1} - X_i\right)\right\} \exp(A_1 \Delta t) - A_0}{A_1} \tag{3.17}$$

where exp is the natural exponential function. If A_1 is zero, Equation (3.17) simplifies to

$$X^n = X_i + A_0 \Delta t \tag{3.18}$$

The criteria represented in Equation (3.16) are also applied in choosing between Equations (3.17) and (3.18). For transient solutions, the travel algorithm is applied once in each time step Δt and the current location recorded for use in the subsequent time step.

4.0 UNCERTAINTY ANALYSIS

Uncertainty analyses are used to quantify uncertainty in model output or model performance measures caused by uncertainties associated with input parameters. A number of different methods can be used to perform uncertainty analyses. First-order and Monte Carlo methods were both used to investigate travel time through Yucca Mountain in this study. Unsaturated zone travel time was selected as the model performance measure.

The first step in the analysis was to evaluate first-order sensitivity coefficients with a deterministic model to rank input parameters used to calculate travel time. The perturbation method (McCuen 1973) was used to determine the sensitivity coefficients. The ranking of input parameters was with respect to their relative importance; parameters with a higher absolute normalized (relative) sensitivity coefficient values were ranked higher. This analysis provided input as to the relative importance of the input parameters that were considered in the uncertainty analysis.

The uncertainty analysis of travel times through Yucca Mountain resulted in estimation of distributions of the unsaturated zone travel time. Uncertainty or variability in the input parameters was propagated through the flow model solution and travel time calculation to generate uncertainty or variability in the output function, the unsaturated zone travel time. For the analysis described in this report, a Monte Carlo version of the PORFLO-3© computer code (PORMC) was applied. The distribution of input parameters was based on the statistical properties of available data collected at Yucca Mountain.

The distribution of unsaturated zone travel time was evaluated for sensitivity to the distributions of the different input parameters. This measure of model sensitivity provided an indication of how much of the variability of travel time was accounted for by each input parameter. The list of parameters contributing the greatest variability by the Monte Carlo method combined with the relative ranking of the sensitivity coefficients determined by the perturbation method provide information on which parameters are important for site characterization.

4.1 SENSITIVITY COEFFICIENTS

First-order sensitivity coefficients quantify the effect of input parameter variation on a model output or performance measure (McCuen 1973). In this study, the perturbation approach was applied to determine sensitivity coefficients.

Let F be a model output parameter or performance measure that is a function of the input parameters $p_1, p_2, \ldots, p_n$. The general definition of a sensitivity coefficient is the derivative

$$S_i = \frac{\partial F}{\partial p_i} \tag{4.1}$$

where S_i is the sensitivity coefficient for the output function F with respect to input parameter p_i. In this study, the performance measure F is UZTT and p_i is one of several input parameters such as recharge rate or hydraulic conductivity. A finite difference approximation to this definition is

$$S_i = \frac{F_2 - F_1}{p_2 - p_1} = \frac{\Delta F}{\Delta p_i} \tag{4.2}$$

where the subscripts 1 and 2 correspond to the state of the system at negative and positive symmetrical variations of p_i about the expected value, respectively. This finite-difference approximation is only meaningful if the sensitivity coefficient is approximately linear in the range of input values considered.

The sensitivity coefficient defined by Equation (4.1) indicates the most influential input parameters p_i with respect to the value of function F. Differences in the magnitudes of parameters make direct comparison of the S_i values difficult. To provide a common basis for comparison, a normalized sensitivity coefficient is defined:

$$Sn_i = \left(\frac{\bar{p}_i}{F(\bar{p}_i)}\right)\left(\frac{\Delta F}{\Delta p_i}\right) \tag{4.3}$$

where $\bar{p}_i$ is the initial (baseline) value of the ith parameter and $F(\bar{p}_i)$ is the value of the output function when all parameters are equal to their baseline values.

Thus, the perturbation approach to estimating sensitivity coefficients consists of repeated simulations with a model while varying the input parameters. The sensitivity coefficient is computed with respect to symmetric positive and negative variation of a input parameter p_i.

4.2 MONTE CARLO METHOD

The Monte Carlo method involves the generation of a statistically large number of "realizations" of input parameters consistent with their statistical distributions. A realization is a single simulation performed by a deterministic model using a particular set of input values, at least some of which are defined stochastically. For each realization a single value of each stochastic variable is randomly sampled from its

assumed probability density function (pdf). The simulation is performed using these values, resulting in a corresponding output variable or model performance measure. By repeating a large number of realizations, a distribution of output variables is developed. The mean, variance, and pdf of the output variable are computed from the output of all realizations performed.

The Monte Carlo method is possibly the most powerful method available for uncertainty analysis because it requires fewer assumptions (e.g., stationarity, the requirement that any statistical property of a variable is stationary in space) compared with other approaches such as the perturbation or spectral methods. The Monte Carlo method is a simple, direct means to translate variation in input parameters into variation in output parameters.

There are several disadvantages to using the Monte Carlo method (de Marsily 1986). First, the method requires a large number of realizations (from 50 to hundreds or thousands) involving a large amount of central processing unit (CPU) time on a computer. This practical limitation was addressed by making use of the assumed steady-state nature of water flow in Yucca Mountain (Montazer and Wilson 1984) to justify the use of steady-state solutions. Solution of a steady-state problem requires much less computational effort than does solution of a comparable transient problem. A second disadvantage is that the method requires knowledge (or assumptions) of the probability distribution of the input variables to be treated stochastically. In this investigation the distributions used to represent stochastic variables were based on data from Yucca Mountain and/or common hydrologic assumptions. A final disadvantage of the method is that the solution is a function of the finite mesh size used. The estimate becomes less variable with increasing mesh size simply because of integration, affecting the variability of the solution. This limitation was addressed by use of a sufficiently small grid mesh to ensure that reasonable solutions were obtained.

5.0 YUCCA MOUNTAIN DATA FOR CALCULATION OF TRAVEL TIME DISTRIBUTION

Examination of the governing equations in Section 3.1 reveals that the data required for calculating travel times with the PORMC code include values for the thickness of geologic units (i.e., the geometry of the problem domain), matrix density, recharge rate, matrix porosity, hydraulic conductivity, and parameters describing unsaturated hydraulic characteristics. All of these except geologic unit thickness and matrix density were treated stochastically in this study. Geologic unit thickness was not treated stochastically because changes in the model grid would have been required. Matrix density was not treated stochastically because it was determined not to be important in the first-order sensitivity analysis (see Section 6.2). Data used to define the statistical nature of these parameters are from the Site Characterization Plan (DOE 1988) and various Yucca Mountain Project documents. In this section, the summary data from the different sources, the resulting stochastic nature of each variable, and the choice of statistical distributions to represent that nature are presented.

Statistical information for the variables treated stochastically in the uncertainty analysis are summarized in Table 5.1. The form of the statistical distribution assumed for each input variable is shown with the first and second moments of the distribution (mean and standard deviation). The statistical distributions are represented as probability density functions (pdfs). The Monte Carlo simulations were conducted with the descriptions of the distributions given in Table 5.1. Together, all the mean values listed in Table 5.1 constitute the baseline case. The baseline case was simulated using the deterministic PORFLO-3© code. The baseline simulation was repeated using PORMC as well, substituting stochastic definitions with a constant distribution specified for each input variable to be treated stochastically. Results of the two simulations were the same, providing a check on the operation of the stochastic modules in the PORMC code.

TABLE 5.1. Summary of Stochastic Variables and Statistical Information for CHnz Unit

Stochastic Parameter	Symbol	Units	Distribution	Mean ($\hat{\mu}$)	Std. Dev. ($\hat{\sigma}$)
Recharge Rate	ln(q)	m d^{-1}	Lognormal	-15.111	2.303
Hydraulic Conductivity	ln(K_S)	m d^{-1}	Lognormal	-14.298	2.050
Total Matrix Porosity	n_T	-	Normal	0.3063	0.0476
van Genuchten alpha	α	m^{-1}	Normal	4.94 x 10^{-3}	6.21 x 10^{-3}
van Genuchten n	n	-	Normal	1.8445	0.6145

A number of statistical distributions were available in the POFIMC code to represent stochastic variables. A variable could be defined with a constant, uniform, loguniform (base e or base 10), normal, lognormal (base e or base 10), or exponential distribution. In addition, actual data could be input as a table to represent the statistical distribution, and variables could be assigned to have linear correlations to other constant or stochastic variables. Use of any statistical distribution requires information to define the center, spread, and skew of the distribution. Only the constant, normal, and lognormal distributions were used in this study, requiring the mean and standard deviation for each variable that was represented stochastically.

5.1 YUCCA MOUNTAIN STRATIGRAPHY

Because of the preliminary nature of this study and the importance of the Calico Hills unit as a natural barrier for the potential repository at Yucca Mountain, we began with a one-dimensional, single-layer model. The single layer chosen for this modeling effort was the Calico Hills nonwelded zeolitic (CHnz) unit.

The thickness of the CHnz unit was modeled after the stratigraphy of the USW-G4 drill hole at Yucca Mountain (Peters et al. 1984) illustrated in Figure 5.1. The CHnz unit lies beneath the potential repository horizon and above the regional water table. The water table is near the lower boundary of the unit, as indicated in Figure 5.1. The CHnz unit is one of the important parts of the natural barrier beneath the potential repository because of the length of time required for water movement through the layer. In all simulations discussed in the report, the CHnz unit was assumed to extend from a depth of 415.0 m to 540.0 m, a thickness of 130-m. The regional water table was assumed to coincide with the bottom of the modeled region, providing the lower boundary condition ($\psi = 0$).

5.2 MATRIX DENSITY

The matrix density (ρ) of a geologic unit is not a parameter in the equations used to calculate travel time and was not expected to affect the travel time results. This hypothesis was tested by treating matrix density stochastically in the first-order sensitivity analysis. Because no effect was anticipated, the sensitivity coefficient should be zero, providing a consistency check on the travel time algorithm. The sensitivity coefficient (reported in Section 6.2) was zero, so the matrix density was not treated stochastically in the Monte Carlo simulations. The matrix density for the CHnz was assumed to have a constant value of 1.654 g cm^{-3}, the arithmetic mean of all available ρ data from the CHnz unit (Table C.1, Appendix C).

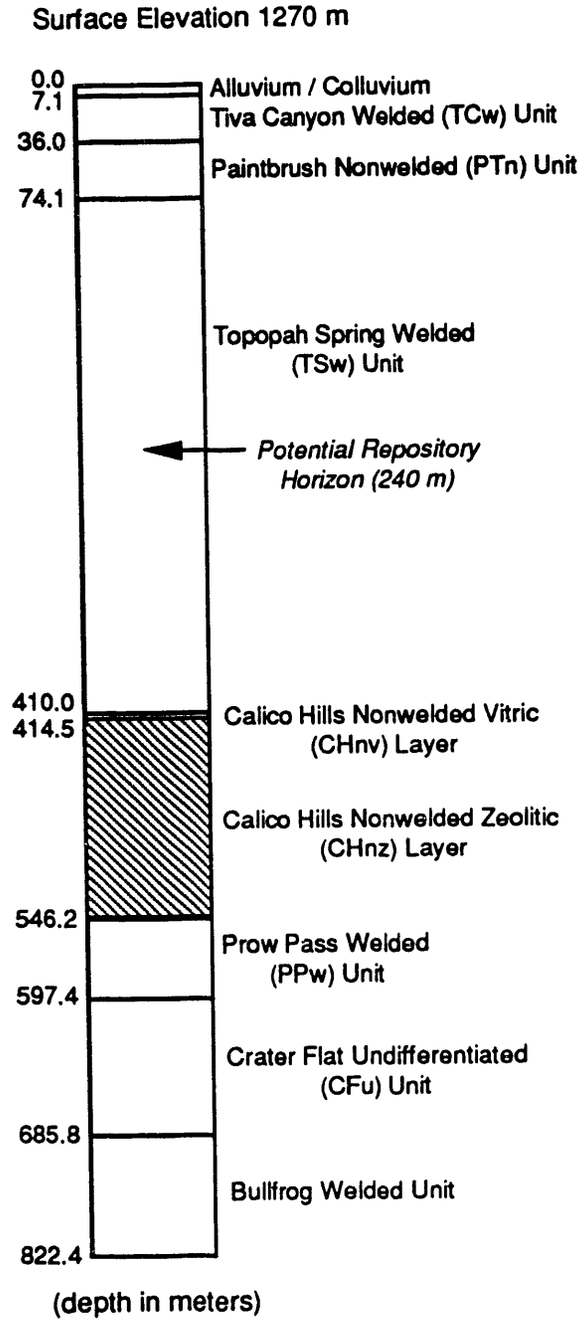

FIGURE 5.1. Generalized Stratigraphy of Drill Hole USW-G4

5.3 RECHARGE RATE

The ultimate source of water in the unsaturated zone at Yucca Mountain is precipitation on the mountain. The recharge resulting from precipitation is both spatially and temporally variable and is difficult to estimate (Montazer and Wilson 1984). It is commonly assumed that natural variations in meteoric water infiltration are damped by the subsurface rock at Yucca Mountain and that the deep percolation, or recharge, is in a steady-state condition at and below the horizon of the potential nuclear waste repository (Lin and Tierney 1986; Jacobson et al. 1986). No direct measurement of moisture flux through the Topopah Springs unit has been made. Available information suggests a steady vertical infiltration flux of less than 0.5 mm y^{-1} beneath the Topopah Springs welded unit (Lin and Tierney 1986; Montazer et al. 1985; Sinnock et al. 1985). The upper bound appears to be around 0.5 mm y-1 (Lin and Tierney 1986).

The statistical distribution selected to represent variation of this parameter was the lognormal (base e) distribution. Although the small number of data available do not directly support this assumption, the lognormal distribution is very robust in representing variation of hydrologic phenomena (Linsey et al. 1982). The baseline value of recharge assumed for this study is 0.1 mm y^{-1}. The variance of the distribution was chosen so that the value of 0.01 mm y^{-1} is two standard deviations below the assumed mean and the value 1.0 mm y^{-1} is two standard deviations above the assumed mean.

5.4 MATRIX POROSITY

The total matrix porosity (n_T) data are from Lin and Tierney (1986). Only seven samples of n_T were available from drill hole USW-G4. To obtain a larger statistical size, samples from all available drill holes (65 samples) were used to compute the summary statistics. These data are summarized in Table C.2 in Appendix C. The histogram (Figure 5.2a) and normal probability plot (Figure 5.2b) indicate that the observed n_T data are approximately normal. Therefore, a normal distribution was used to describe variation in total matrix porosity. The mean and standard deviation computed from the available data in Table C.2 (Appendix C) for the CHnz unit was used to describe the center and spread of the assumed normal distribution.

It was not possible to define the residual moisture content (θ_R) as a random variable in this study because of the input requirements and nature of PORFLO-3© and PORMC. Porosities (n_E, n_T), rather than θ_R and θ_S, are entered for these codes. Therefore, we could define n_T and n_E stochastically, but not θ_R which is equal to $n_T - n_E$. However, if we define both n_T and n_E stochastically, it would be possible for n_E to be greater than n_T. Such an occurrence would violate the strict definition of these porosities ($n_E \leq n_T$). For this reason, only n_T was treated stochastically. In each simulation the value of n_E was obtained by subtracting the arithmetic mean of θ_R (calculated from the data in Table C.3 in Appendix C) from the stochastically generated value of n_T.

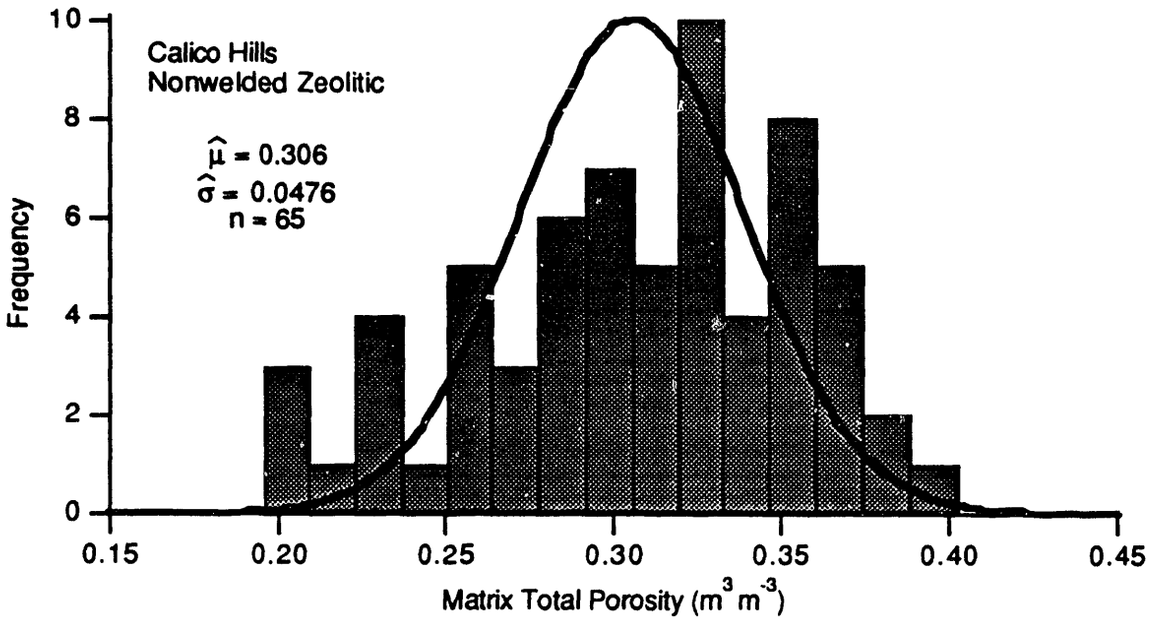

a) Frequency Histogram

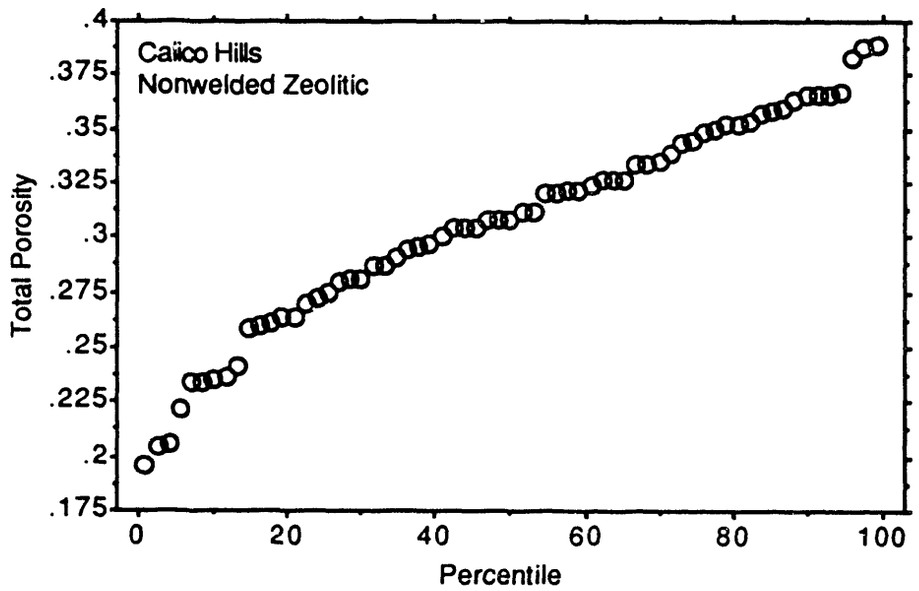

b) Normal Probability Plot

FIGURE 5.2. Statistical Distribution of Matrix Total Porosity Data for CHnz Unit (Peters et al. 1984)

5.5 HYDRAULIC CONDUCTIVITY

To represent the variation of saturated hydraulic conductivity (K_S) across orders of magnitude observed at Yucca Mountain, the lognormal distribution (base e) was chosen. Available saturated hydraulic conductivity data are listed in Table C.4 of Appendix C. Figure 5.3a shows the frequency distribution of lognormal hydraulic conductivity for the available data from the CHnz unit (Peters et al. 1984); Figure 5.3b shows the normal probability plot for these data. The lognormal distribution appeared to adequately model the stochastic nature of K_S in the CHnz unit. Lin and Tierney (1986) applied the same assumption with regard to the variation of hydraulic conductivity in their preliminary estimation of travel time distribution through Yucca Mountain.

5.6 UNSATURATED HYDRAULIC CHARACTERISTIC PARAMETERS

The van Genuchten parameters (van Genuchten 1978) are empirical curve-fitting terms used in relating pressure head (P), expressed as soil moisture potential (ψ), with moisture content (θ) and hydraulic conductivity (K_x, K_y, K_z) for unsaturated flow. The van Genuchten relationship for moisture content is

$$\theta = \theta_R + (\theta_S - \theta_R)(1 + (\alpha\psi)^n)^{-m} \qquad (5.1)$$

where α, m, and n are curve-fitting parameters, θ_S is the moisture content at saturation, and θ_R is the residual moisture content. It is assumed that m = 1-1/n. We used Mualem's predictive model (van Genuchten 1978, van Genuchten 1980, Mualem 1976) for the relationship for hydraulic conductivity:

$$K = K_S\,\theta^{1/2}\left[1 - (1 - \theta^{-m})^m\right]^2 \qquad (5.2)$$

where K is the (unsaturated) hydraulic conductivity (K_x, K_y, or K_z) and K_S is the saturated hydraulic conductivity. The fitting parameters α and n are the empirical curve-fitting parameters treated stochastically in this study.

There were an insufficient number of α and n data to make any strong conclusions about the underlying statistical distributions of these parameters. A normal distribution was assumed to be appropriate for both, based on the distribution of available α and n data for the CHnz unit of Yucca Mountain summarized in Table C.5 of Appendix C. The mean and standard deviation were computed from available data sampled from drill hole USW-G4 at Yucca Mountain.

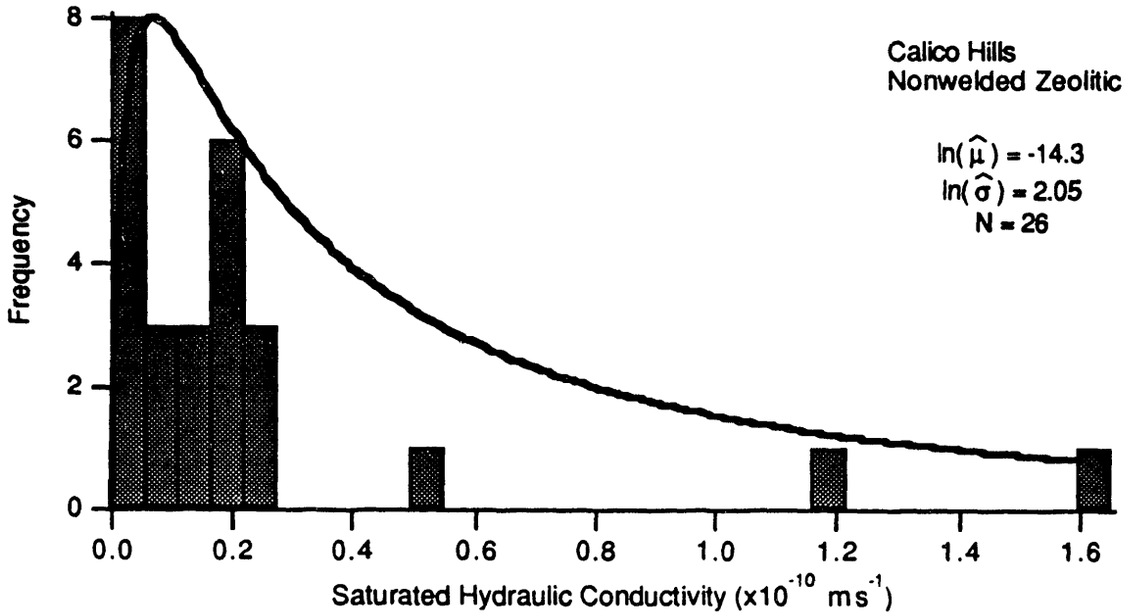

a) Frequency Histogram

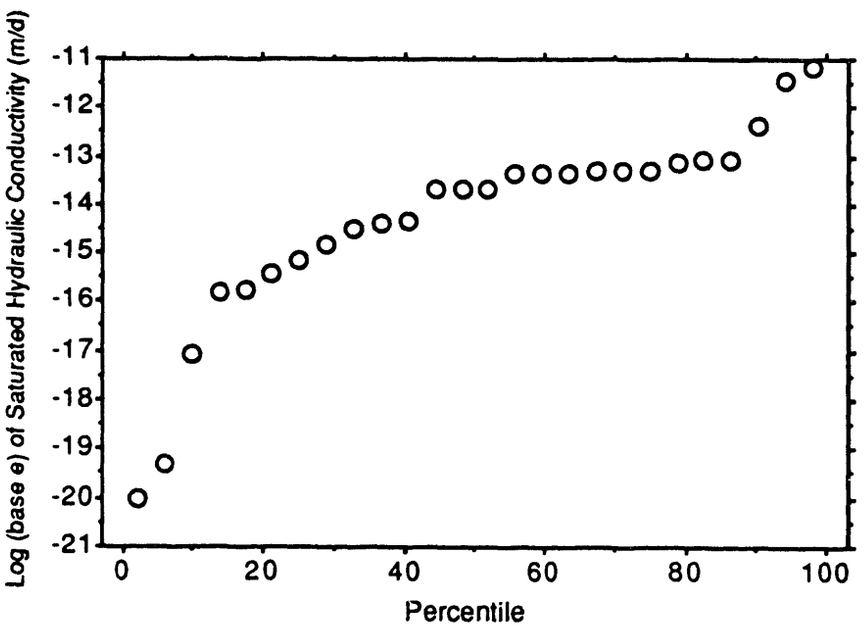

b) Normal Probability Plot

FIGURE 5.3. Statistical Distribution of Hydraulic Conductivity Data for CHnz Unit

The range of α and n must be restricted to physical bounds for random sampling procedures and selection of perturbation values. The lower boundary of α is zero; if α is less than or equal to zero the relationship between θ and ψ becomes a vertical line, and is no longer representative of a true physical system. For n, the lower boundary is 1.0. Values of n less thar .ıe specify a relationship in which θ increases, rather than decreases, with increasing ψ (a physical impossibility).

6.0 COMPUTATIONAL RESULTS AND ANALYSIS

This section presents results and analysis for the sensitivity and uncertainty analyses of water travel time through the unsaturated zone at Yucca Mountain. The baseline case, a deterministic simulation of water travel time using the baseline value of each variable as a constant, is described in Section 6.1. Section 6.2 covers the computation of sensitivity coefficients in the first-order sensitivity analysis and ranking of input parameters based on their effect on UZTT. Section 6.3 contains a description of the results of Monte Carlo simulations involving single stochastic input variables. Section 6.4 provides the results of the uncertainty analysis based on a fully stochastic simulation in which all input parameters are defined stochastically. Finally, all of these results are compared with the findings of other researchers in Section 6.5.

6.1 BASELINE CASE

The baseline case consisted of a single deterministic simulation against which the results of all simulations for the sensitivity and uncertainty analyses were compared. The baseline value of each parameter was the mean for parameters represented by normal (symmetrical) distributions or the median for parameters represented by lognormal (non-symmetrical) distributions (i.e., recharge rate and saturated hydraulic conductivity). In subsequent simulations involving variation of only a single parameter, the remaining parameters were held constant at their baseline values.

The values of input parameters used for the baseline case are summarized in Table 6.1. The computed travel time for the baseline simulation was 8.534×10^7 days, or approximately 233,539 years. Relative saturation in the 130-m thick unit ranged from approximately 0.88 at the upper boundary to 1.0 at the lower boundary (water table) for the steady-state simulation. Figure 6.1 shows the travel time versus depth in the simulation domain (the CHnz unit). Because the range of saturations is narrow, the travel time profile mapped by these ten points is nearly linear, though such a curve can be non-linear depending on the unsaturated conditions of the profile.

The baseline simulation was performed with the PORFLO-3© version 1.1 code. It was repeated using the PORMC version 1.0 code to provide a check on the operation of the stochastic modules. In the repeated simulation, a constant distribution (variance equal to zero) was specified for the five input

TABLE 6.1. Input Parameter Values For Baseline Simulation

	q ($mm\ y^{-1}$)	K_S ($m\ d^{-1}$)	ρ ($kg\ m^{-3}$)	n_r	α (m^{-1})	n
Baseline Value	0.10	6.172×10^{-7}	1.654	0.3063	4.94×10^{-3}	1.8445

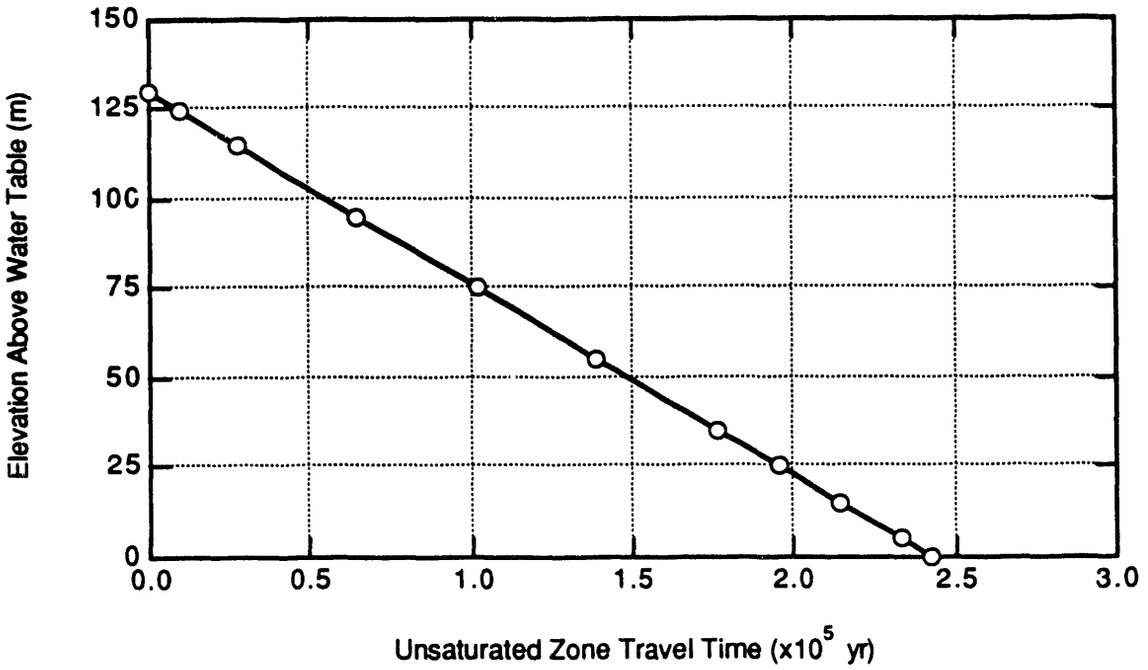

FIGURE 6.1. Baseline Case Travel Times at Various Depths

variables of interest. This permitted PORMC to produce numerical results that could be compared to those obtained with PORFLO-3©. The simulation results for the two codes were identical.

6.2 SENSITIVITY ANALYSIS

Computing the sensitivity coefficients in the first-order sensitivity analysis required two simulations for each parameter; one positive and one negative perturbation relative to the baseline case discussed in Section 6.1. The perturbation values used for each simulation are listed in Table 6.2. Only the diagonal terms (perturbed values) are shown for clarity; the off-diagonal terms are the baseline values given in Table 6.1. Most parameters were perturbed by ±50%, but some were varied less for physical reasons associated with each parameter.

Simulations with the parameter values in Tables 6.1 and 6.2 resulted in the travel times and the sensitivity coefficients listed in Table 6.3. Recall that one of the six parameters, matrix density (ρ), was included as a check on the flow code and travel time algorithm. Because variation of ρ should have no effect on computed travel time the sensitivity coefficient should be zero for this parameter. The values in Table 6.2 for the matrix density sensitivity coefficients are zero, as expected. The other five parameters show varying degrees of importance as reflected in the normalized sensitivity coefficients (Sn_i); matrix porosity is the most influential variable, followed by recharge rate.

TABLE 6.2. Input Parameter Values For Perturbation Simulations

Simulation		q ($mm\,y^{-1}$)	K_S ($m\,d^{-1}$)	ρ ($kg\,m^{-3}$)	n_T	α (m^{-1})	n
q	High	0.23					
	Low	0.044					
K_S	High		1.391×10^{-5}				
	Low		2.738×10^{-7}				
ρ	High			1.9021			
	Low			1.4059			
n_T	High				0.4595		
	Low				0.1532		
α	High					7.41×10^{-3}	
	Low					2.47×10^{-3}	
n	High						2.3978
	Low						1.2911

TABLE 6.3. Sensitivity Coefficients

Parameter	High Perturbation, d	Low Perturbation, d	S_i	S_{ni}
Baseline	88,485,824			
Recharge	39,752,860	195,634,320	-8.61×10^{8}	-0.9733
Conductivity	86,823,392	85,720,392	9.87×10^{11}	0.0069
Matrix Density	88,485,824	88,485,824	0.0	0.0
Total Porosity	160,401,070	16,617,496	4.69×10^{8}	1.6249
van Genuchten α	87,943,800	89,197,976	-2.54×10^{8}	-0.0142
van Genuchten n	88,705,480	89,480,768	-7.01×10^{5}	-0.0146

6.3. SINGLE-VARIABLE STOCHASTIC SIMULATIONS

A series of single stochastic simulations provided detailed information on how each variable affects travel time for the conditions in the CHnz geologic unit. In these simulations, a single variable was treated stochastically while all other variables were held constant at their baseline values (Table 6.1). Each stochastic variable was sampled from the assumed pdf for that variable (see Table 5.1). Because each parameter has a distinct travel time response, the responses are discussed separately in Sections 6.3.1 through 6.3.5.

6.3.1 Recharge Rate

Variation of the recharge rate (q) based on its assumed lognormal distribution resulted in a linear response in UZTT, as illustrated in Figure 6.2. Figure 6.2a shows the 50 realizations of the recharge rate plotted against the corresponding travel time. Figure 6.2b shows the same information as a cumulative distribution. The range of travel time spans more than an order of magnitude resulting from uncertainty in the recharge rate. Because recharge is a multiplicative factor in Equations (3.10) and (3.11) used to compute travel time, the linear behavior illustrated in Figure 6.2 is expected, provided the recharge rate does not exceed the saturated hydraulic conductivity. In the event that the recharge rate is greater than the saturated hydraulic conductivity, the profile would be saturated and travel time could be directly computed by dividing the distance traveled by the darcian flux rate in that direction, i.e., Δz / W. Because our one-dimensional conceptual model could not address ponding above the profile, this event was assumed not to occur.

6.3.2 Hydraulic Conductivity

Uncertainty in saturated hydraulic conductivity (K_S), represented by an assumed lognormal distribution, produced a nearly linear response in travel time (Figure 6.3). Figure 6.3a shows the 50 realizations of travel time plotted against the resulting travel time values, and Figure 6.3b shows the cumulative frequency distribution for travel times resulting from variation of K_S. As mentioned in Section 6.3.1, recharge must be less than saturated hydraulic conductivity for the one-dimensional simulation to be applicable. The non-linearity in the travel time response is caused by the non-linearity inherent to the unsaturated hydraulic conductivity relationship (Sections 5.6, 6.3.4, and 6.3.5). The range of travel time is narrow, indicating that variation of the saturated hydraulic conductivity does not have a large affect on travel time for the conditions modeled. This is reasonable because it is the unsaturated hydraulic conductivity that is used to calculate travel time, therefore parameters that describe the unsaturated relationship should be more important than the saturated values themselves.

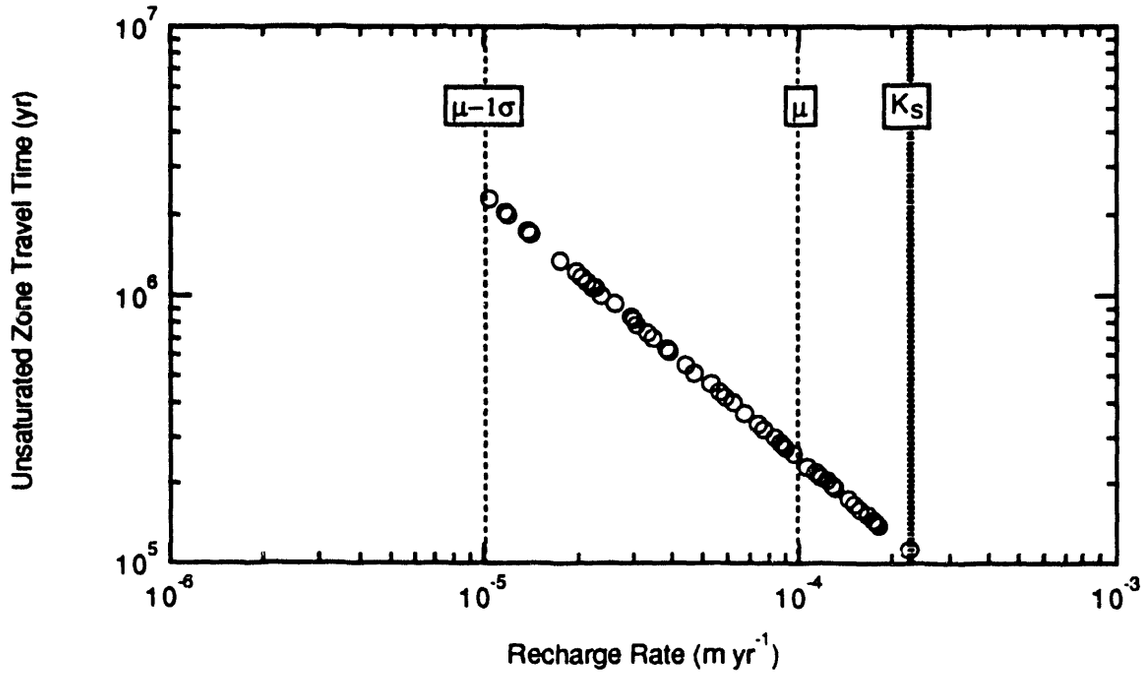

a) Scatter Plot

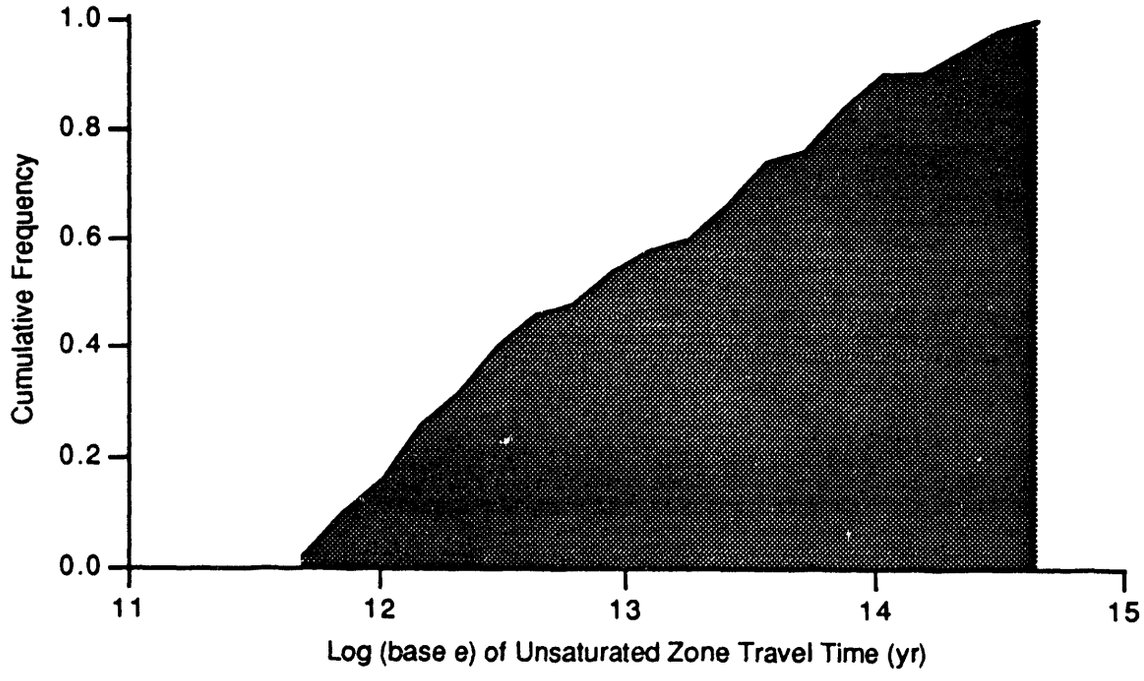

b) Cumulative Distribution

FIGURE 6.2. Travel Time Response to Recharge Rate Variation

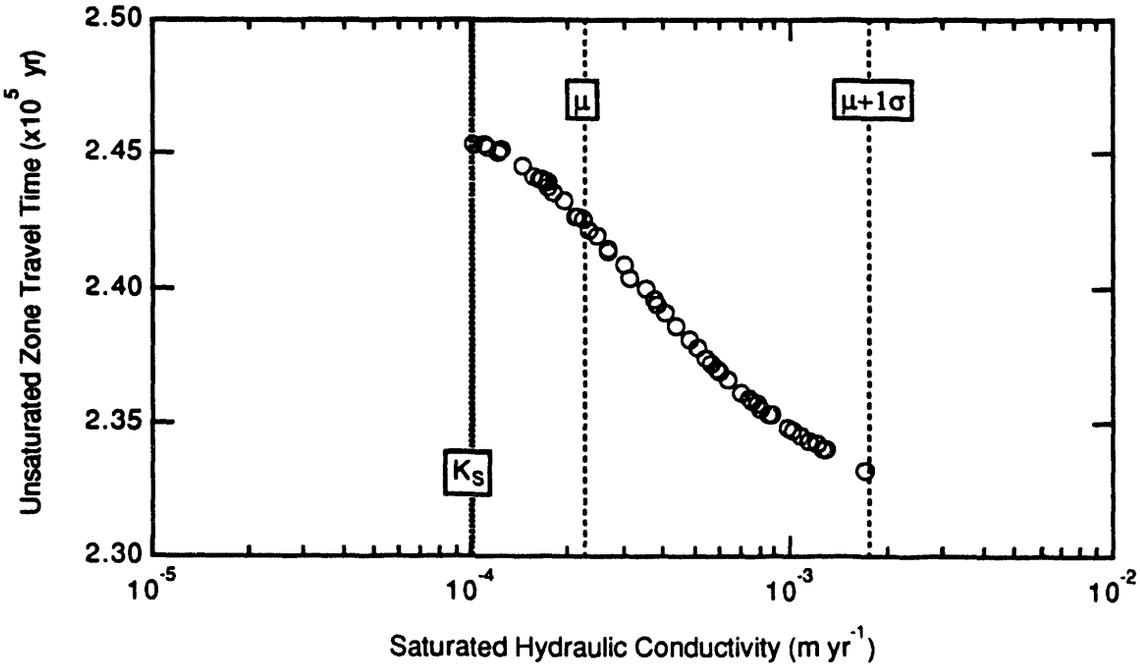

a) Scatter Plot

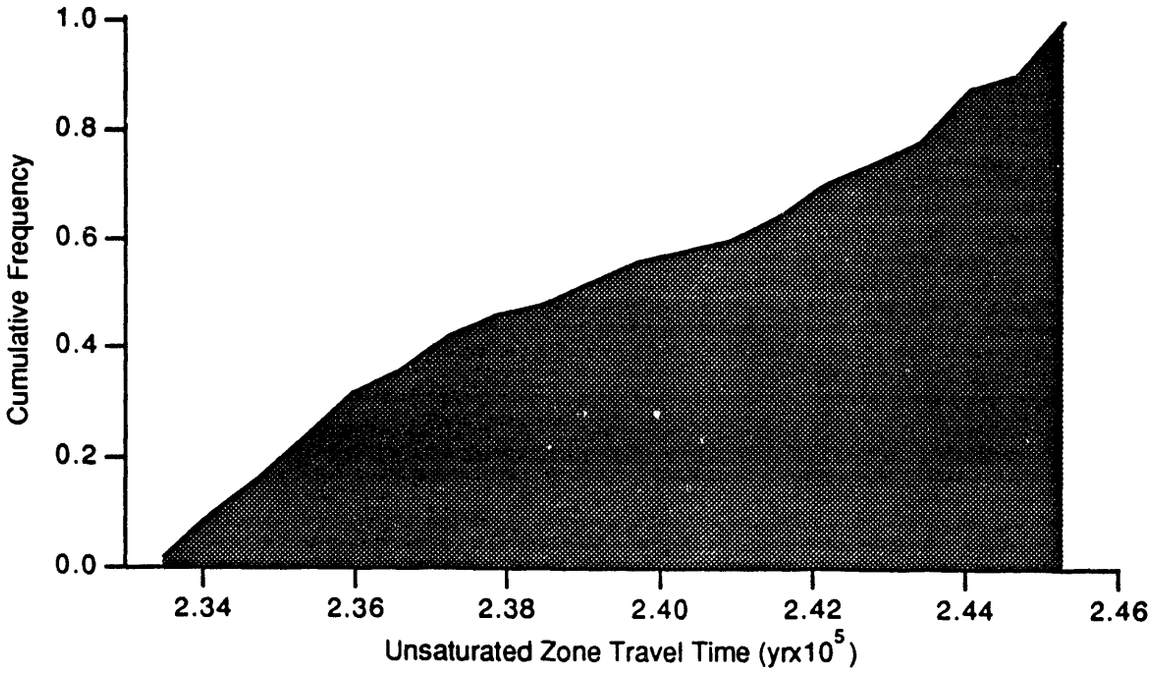

b) Cumulative Distribution

FIGURE 6.3. Travel Time Response to Saturated Hydraulic Conductivity Variation

6.3.3 Matrix Porosity

Uncertainty in matrix porosity represented by a normal distribution produced a positive linear response in travel time (Figure 6.4). Similar to recharge rate, porosity is a direct multiplier in Equations (3.10) and (3.11) used to compute the unsaturated zone travel time; hence, the linearity in the response curve was expected. The range of travel time spans nearly an order of magnitude, indicating that matrix porosity, represented by effective porosity in Equations (3.10) and (3.11), has a greater effect on travel time than saturated hydraulic conductivity. Effective porosity (n_E) was coupled to total porosity (n_T) in each simulation by defining $n_E = n_T - \theta_R$ for each realization, where θ_R is the mean value of residual saturation for the CHnz unit. Residual saturation data are listed in Table C.5 in Appendix C.

6.3.4 van Genuchten α Term

The van Genuchten alpha (α) parameter was sampled from a normal distribution (Table 5.1) truncated at its lower physical limit of zero. The response in travel time was mildly non-linear, particularly near the lower bound. Figure 6.5 shows the travel time response for the 50 realizations of α that were simulated. The range of the travel time response represented by the vertical axes in Figures 6.5a and 6.5b is narrow, indicating that α does not have a large effect on travel time.

6.3.5 van Genuchten n Exponent

The van Genuchten n exponent was sampled from a normal distribution (Table 5.1) truncated at the lower end by the physical limit of one. A value of n less than one would imply that soil moisture content increases with soil moisture tension, which is physically unreasonable. The response of travel time to variation of n was highly non-linear. Figure 6.6a illustrates the parabolic shape of the response curve. Unsaturated zone travel time is not a monotonic function of n. This non-monotonic behavior follows the fact that n is an exponent in the unsaturated hydraulic characteristic relationships.

The applicability of the sensitivity coefficients for n reported in Table 6.2 are questionable in light of the shape of the response curve shown in Figure 6.6. Because the sensitivity coefficient was computed from a finite difference approximation to the derivative of the curve depicted in Figure 6.6a, the approximation only holds if the curve is approximately linear. Because the slope and sign of the derivative change across the range of interest, the sensitivity coefficient for n given in Table 6.3 is not meaningful.

6.4 SIMULTANEOUS MULTI-VARIABLE STOCHASTIC SIMULATION

A simultaneous multi-variable simulation was performed to obtain the response curves and cumulative distribution function (cdf) of travel time resulting from uncertainty in all five input parameters. This simulation was performed for 70 realizations. More realizations were performed for the multi-variable simulation than for the single-variables simulations because the randomly chosen values of recharge rate

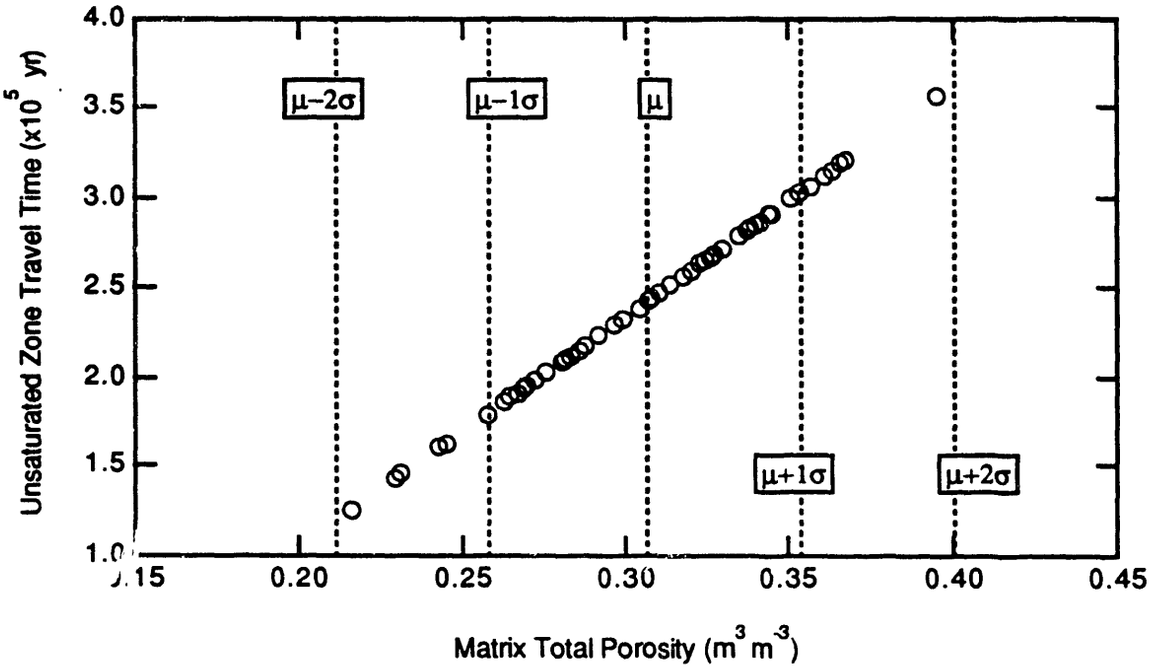

a) Scatter Plot

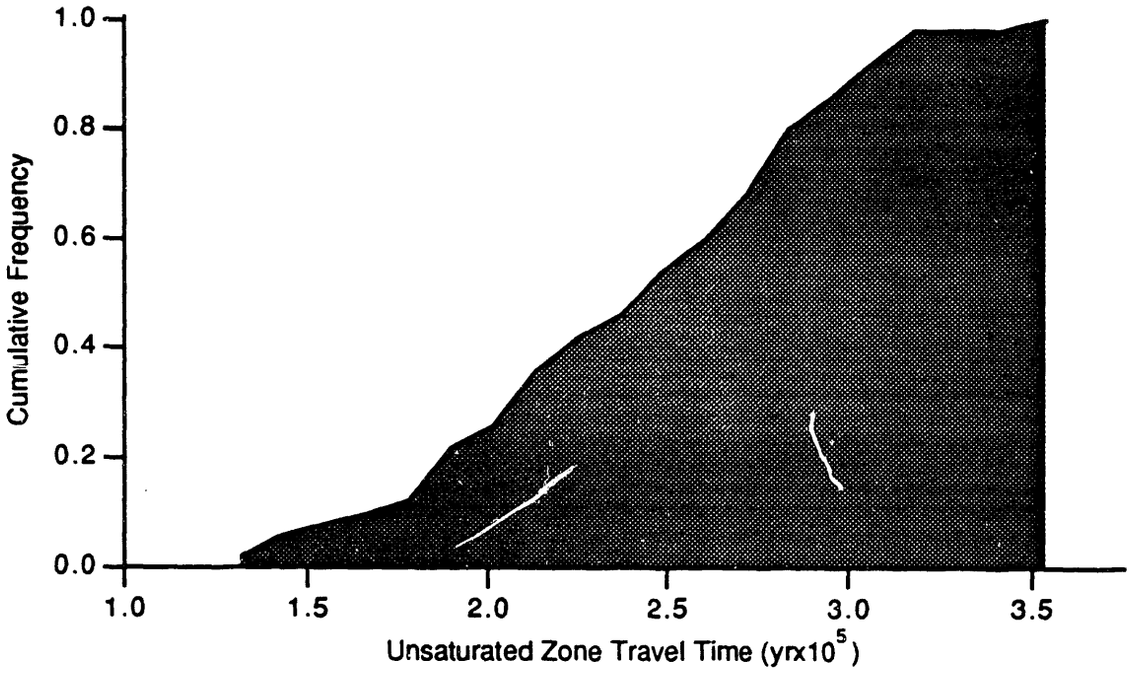

b) Cumulative Distribution

FIGURE 6.4. Travel Time Response to Matrix Total Porosity Variation

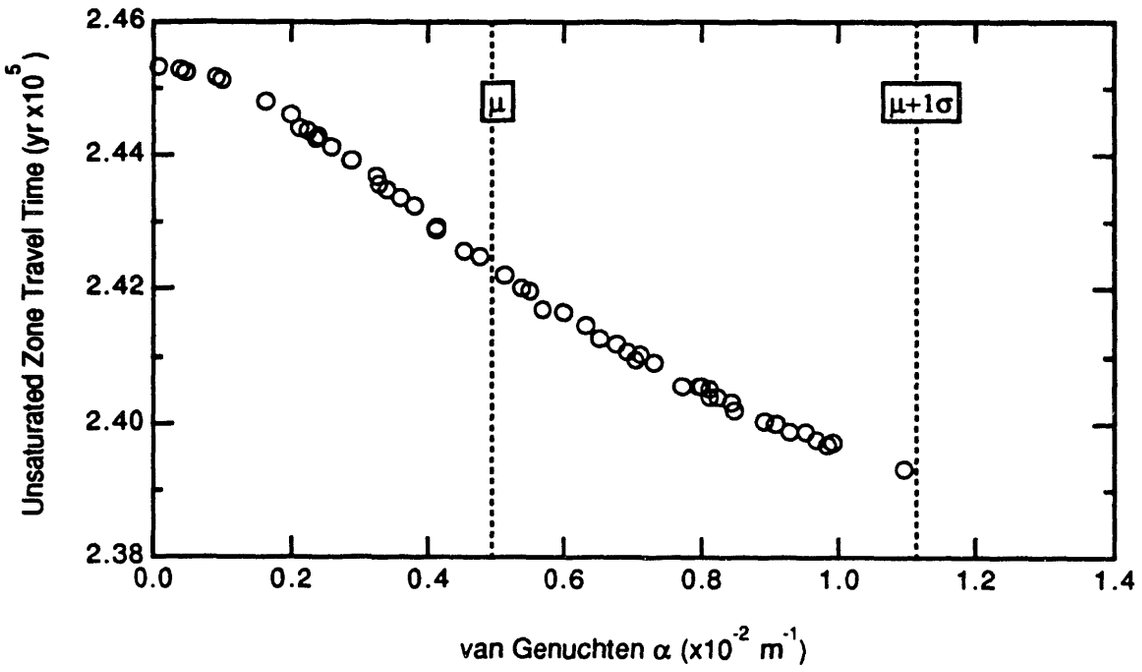

a) Scatter Plot

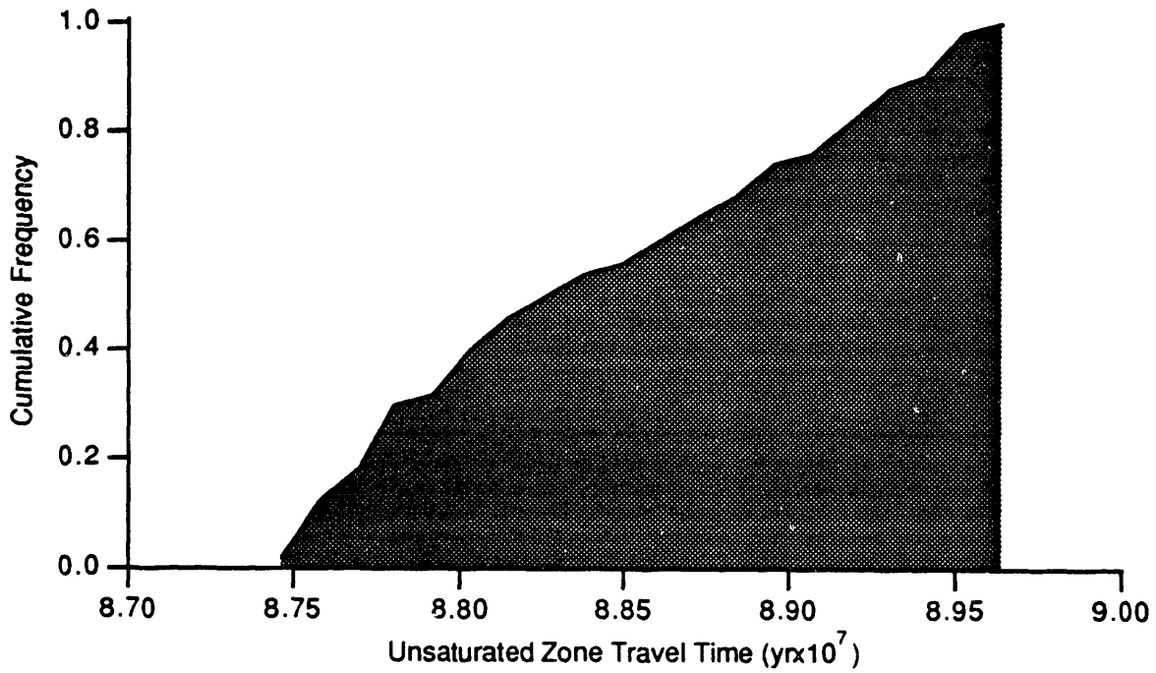

b) Cumulative Distribution

FIGURE 6.5. Travel Time Response to van Genuchten α Variation

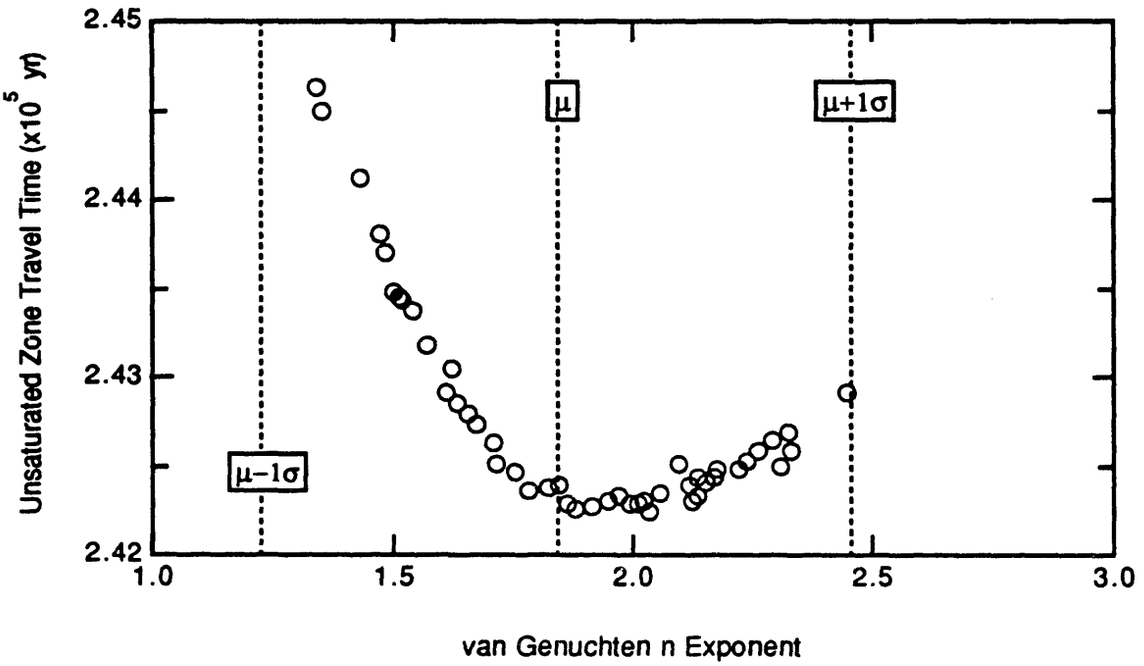

a) Scatter Plot

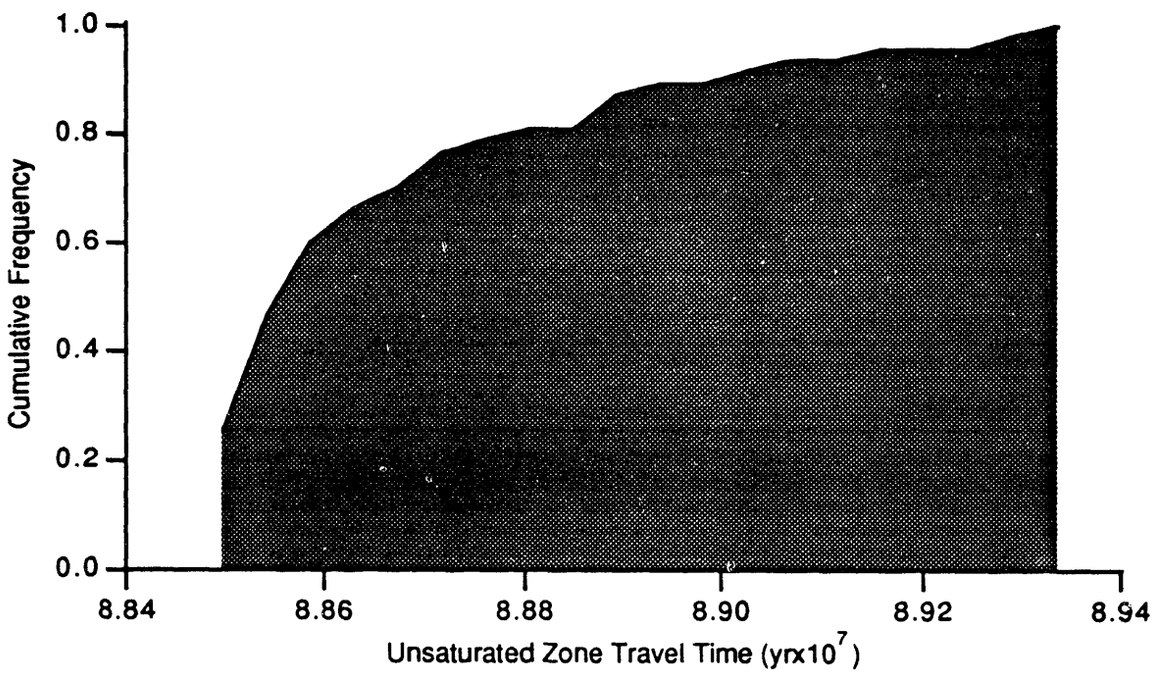

b) Cumulative Distribution

FIGURE 6.6. Travel Time Response to van Genuchten n Exponent Variation

and saturated hydraulic conductivity were expected to occasionally violate the required unsaturated condition. Also, it was anticipated that some combinations of input parameters would result in solutions that would exceed the prescribed number of iterations and/or the convergence criteria specified during solution by the PORMC code. Of the 70 realizations attempted, 67 realizations produced values for use in the analysis, 2 realizations produced values violating the unsaturated condition, and 1 realization could not be solved within the computational limits imposed.

Figure 6.7 shows the response of travel time resulting from the multi-variable stochastic simulation. The histogram (Figure 6.7a) and the cumulative frequency distribution (Figure 6.7b) are shown. Note the logarithmic scale for travel time (horizontal axis in Figure 6.7a). Because of the predominant influence of the recharge rate, the final output response curve strongly resembles the response curve for variation of recharge rate alone. The travel times resulting from the 67 realizations ranged over approximately two orders of magnitude. The uncertainty in recharge contributes at least one order of magnitude to the variation in travel time (Section 6.3).

To illustrate the influence of each parameter in the simultaneous multi-variable stochastic simulation, each parameter was plotted against UZTT (Figures 6.8 through 6.12). In these figures, the travel time from each realization is plotted against the respective input variable randomly chosen for the realization. Other than for the recharge rate (Figure 6.8) no discernable trend was present, indicating that uncertainty in recharge produces the greatest effect on the travel time distribution.

A multiple regression analysis was made between all five input variables (q, K_S, n_T, α, and n) and UZTT in order to examine each variable's contribution to the overall uncertainty in travel time for the simultaneous multi-variable stochastic simulation. The coefficients (β values) of regression are summarized in Table 6.4, along with other statistics obtained from the regression analysis. As observed by examining the results graphically, the regression analysis shows that a large portion of the variation explained by recharge rate alone. To illustrate, a simple linear regression model between the recharge rate and resultant travel time gives a coefficient of determination (r^2) equal to 0.896, meaning that using recharge only explains 89.6% of the variability in the travel time calculation. As seen in Table 6.4, a multiple regression using all five stochastic variables improves the fit of the linear model modestly (r^2 = 0.961). The one-way analysis of variance summarized in Table 6.4 indicates that the multiple regression model accounts for a significant portion of the variance (F = 299.3 with 5,61 degrees of freedom; P-value < 0.001).

The reason for using multiple regression is to enable analysis of each input variable's contribution to the uncertainty in the travel time calculation. This is accomplished through use of the partial F statistics listed in Table 6.4. If the partial F value is significant, it identifies a variable that is statistically significant given that all other independent variables have been included in the model (Weisberg 1985).

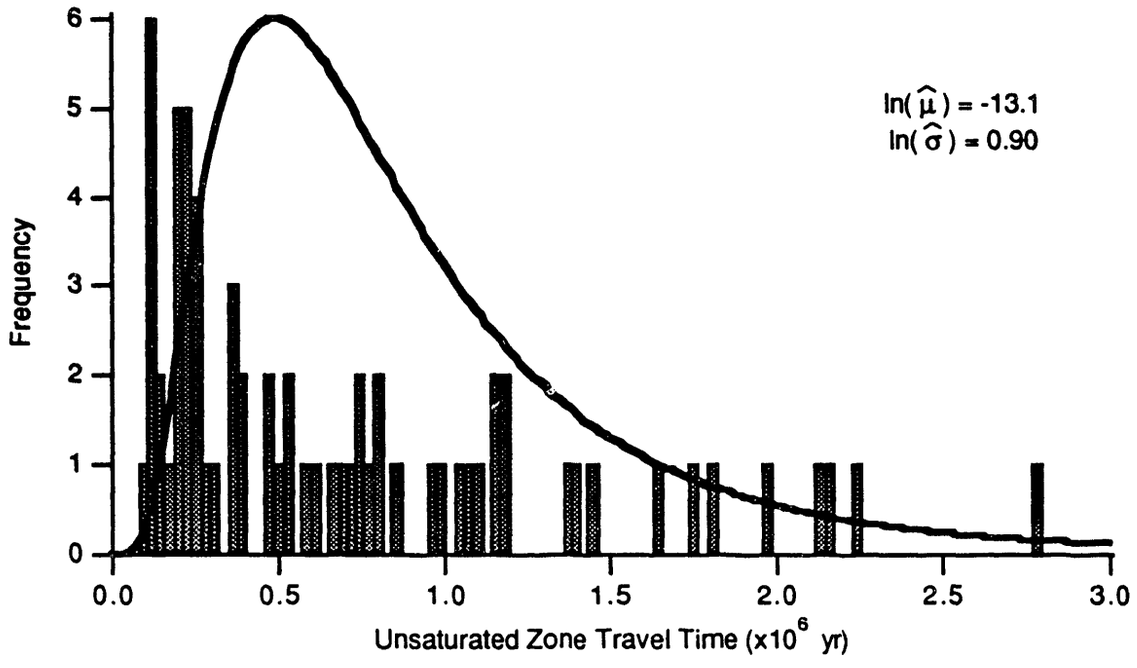

a) Histogram

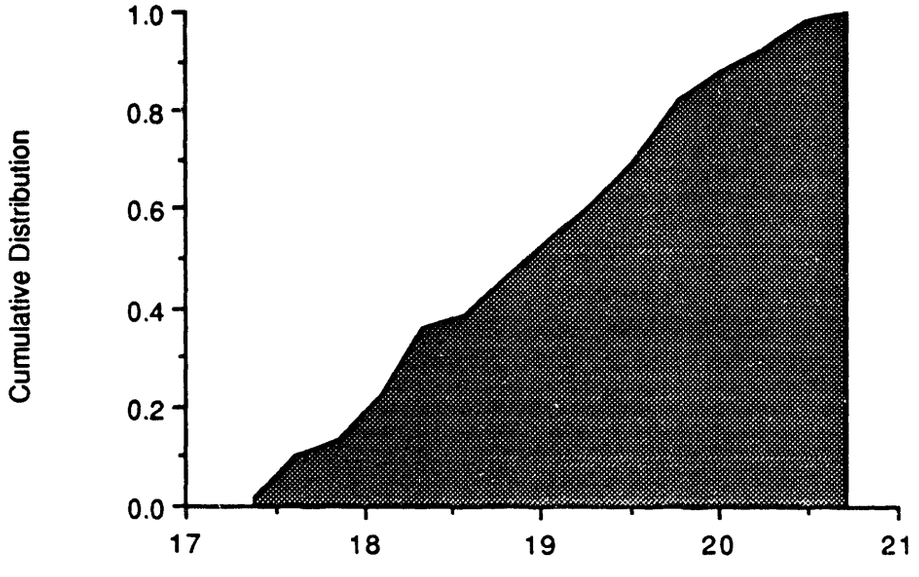

b) Cumulative Distribution

FIGURE 6.7. Travel Time Response to Simultaneous Multiple Parameter Variation

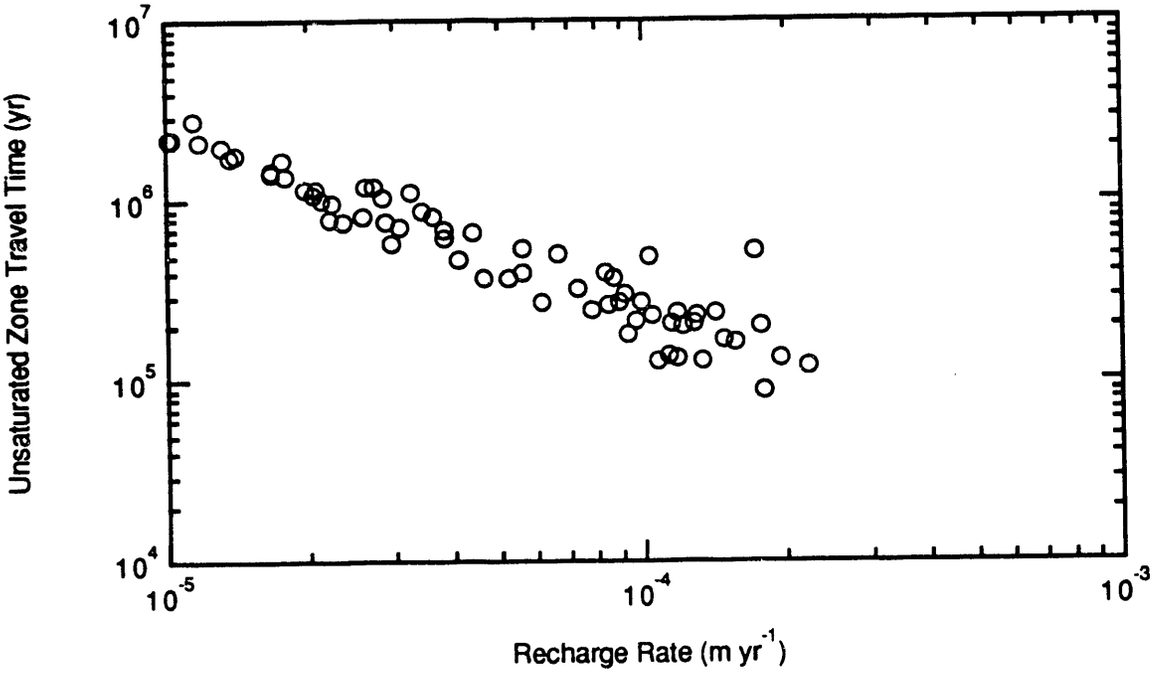

FIGURE 6.8. Recharge Rate Versus Travel Time for Multi-Variable Stochastic Simulation

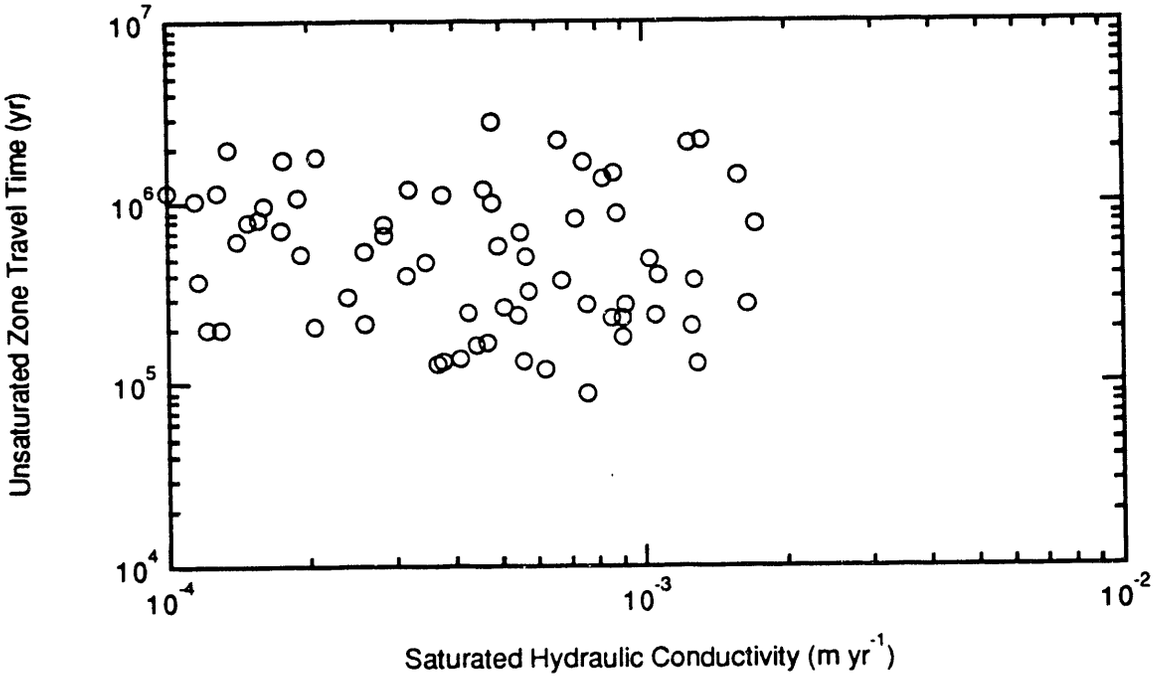

FIGURE 6.9. Hydraulic Conductivity Versus Travel Time for Multi-Variable Stochastic Simulation

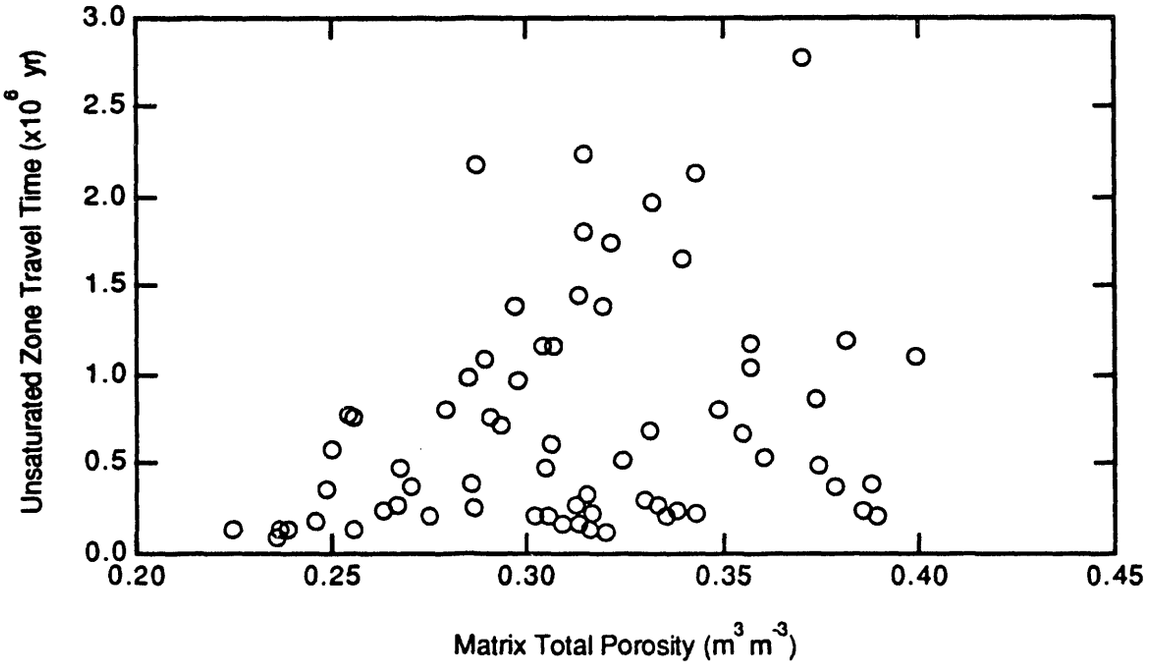

FIGURE 6.10. Total Porosity Versus Travel Time for Multi-Variable Stochastic Simulation

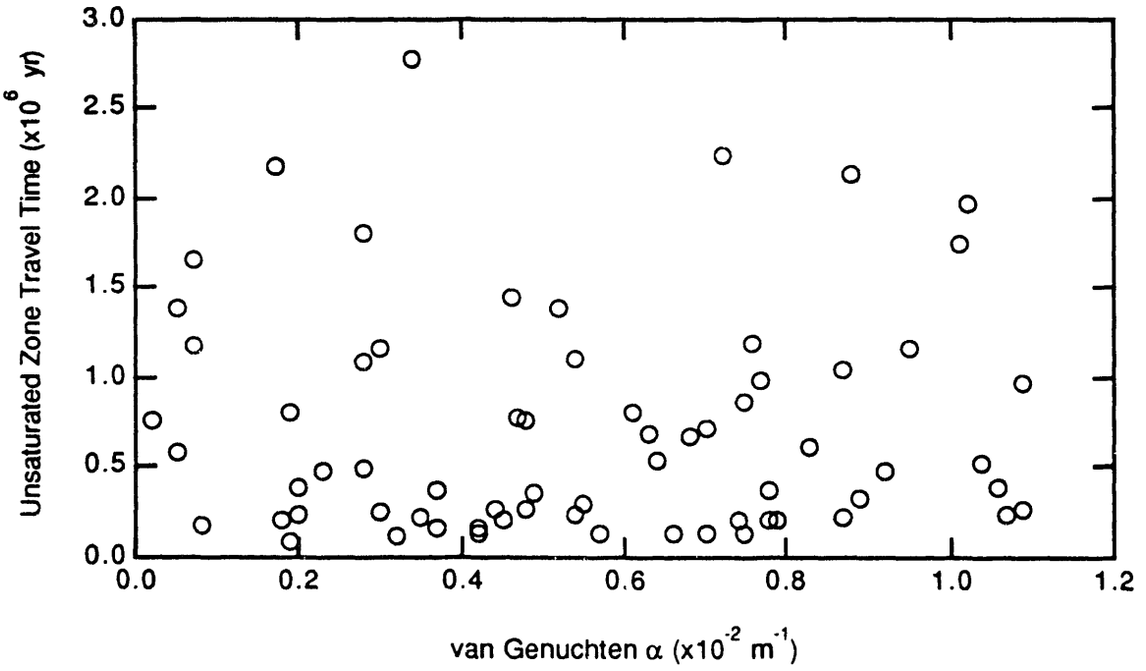

FIGURE 6.11. van Genuchten α Versus Travel Time for Multi-Variable Stochastic Simulation

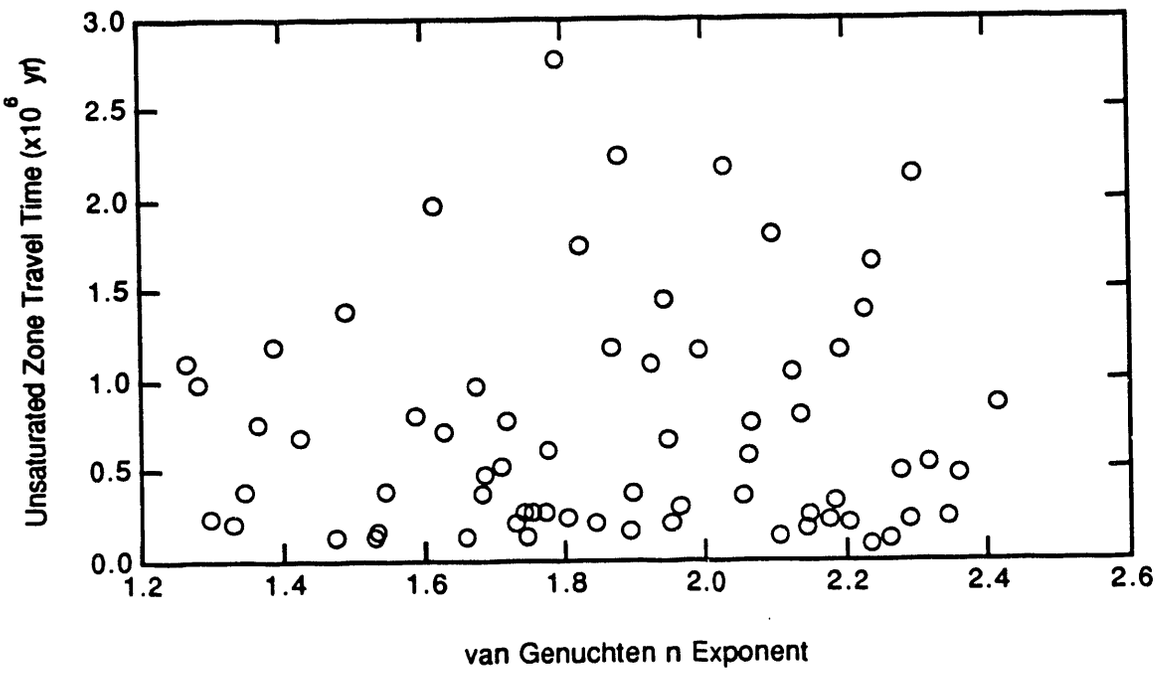

FIGURE 6.12. van Genuchten n Versus Travel Time for Multi-Variable Stochastic Simulation

Conversely, if the partial F value is not significant, then the addition of the respective parameter does not significantly contribute to the predictable variance. From Table 6.4 only two parameters are significant; recharge rate (partial F = 1303 with 1 and 61 degrees of freedom; P-value < 0.0001) and matrix porosity (partial F = 87.21 with 1 and 61 degrees of freedom; P-value < 0.0001). Saturated hydraulic conductivity, van Genuchten's α, and van Genuchten's n are not statistically significant to the multiple regression model. Thus, the recharge rate is the single most important parameter in terms of unsaturated zone travel time uncertainty, followed by the matrix porosity.

6.5 COMPARISON WITH OTHER RESEARCHERS

Previous researchers have conducted sensitivity and uncertainty analyses with information from Yucca Mountain. Jacobson et al. (1985) performed first-order sensitivity and uncertainty analyses on travel time through the unsaturated zone at Yucca Mountain. In their analysis, they used a one-dimensional, steady-state, analytic solution for unsaturated flow and a finite difference approximation for the travel time calculation. A form of their solution is presented in Appendix B and was used to verify the travel time calculations performed by PORFLO-3© and PORMC.

Jacobson et al. (1985) evaluated sensitivity coefficients for unsaturated zone travel time with respect to different ranges of variation in the recharge rate. They determined that the sensitivity

TABLE 6.4. Analysis of Variance for Multiple Regression of Input Parameters on Travel Time

Analysis of Variance Table

Source	d.f.	Sum Squares	Mean Square	F-test
Regression	5	51.375	10.275	299.3
Residual	61	2.094	0.034	p = 0.001
Total	66	53.468		

Count	r	r^2	Adjusted r^2	RMS Residual
67	0.980	0.961	0.958	0.185

Beta Coefficient and Partial F Table

Variable	Coefficient	Std. Err.	Std. Coeff.	t-value	Prob.	Partial F
Intercept	1.805					
ln(q)	-0.955	0.260	-0.929	36.102	0.0001	1303.0
$\ln(K_S)$	-0.026	0.030	-0.023	0.870	0.3877	0.757
n_T	5.157	0.552	0.248	9.339	0.0001	87.21
α	-5.767	8.006	0.019	0.720	0.4741	0.519
n	0.530	0.074	0.019	0.718	0.4754	0.516

coefficient varied with the assumed range of variation in the recharge rate. In the sensitivity analysis presented in this report, normalized sensitivity coefficients were considered to eliminate the effect of different ranges of variation in the input parameters on the resulting sensitivity. This was done so that the relative sensitivity coefficients could be compared among the different input parameters.

Jacobson et al. (1985) also performed a first-order uncertainty analysis for recharge and saturated hydraulic conductivity. The first-order uncertainty analysis was derived from a Taylor series expansion neglecting second order and higher terms. Because the range of recharge rates from available data was not symmetric about the mean, they assumed a lognormal distribution. They also assumed a lognormal distribution for hydraulic conductivity. In their analysis, hydraulic conductivity was predicted to produce much less variation in travel time than recharge rate, which is consistent with the uncertainty analysis presented in this report.

Lin and Tierney (1986) developed a probabilistic method for calculating the ground-water travel time

from the repository horizon to the water table. As in this study, they assumed vertically downward, steady-state flow in the unsaturated zone below the repository horizon. However, unlike in this study, they also assumed a unit gradient condition ($\partial h/\partial z = -1$), a restriction which implied that fluid flow was assumed to be driven solely by the elevation head in the direction of gravity. The unit gradient assumption permitted development of a less rigorous mathematical formulation for unsaturated zone travel time than the one applied by the PORFLO-3© and PORMC codes for this investigation. Lin and Tierney (1986) treated three parameters stochastically; saturated hydraulic conductivity, effective matrix porosity, and fracture porosity. They did not treat the unsaturated hydraulic characteristic curve-fitting parameters stochastically. As in this study, Lin and Tierney (1986) assumed all input parameters were statistically independent from one another. To address recharge rate variation, they chose three values to use in their simulations for contrast. The values were 0.1 mm yr^{-1}, 0.5 mm yr^{-1} (baseline case), and 1.0 mm yr^{-1}. In contrast to the one-dimensional, single-unit simulations discussed in this report, Lin and Tierney (1986) examined travel time for the three stratigraphic units between the repository horizon and the water table, and applied a quasi-three dimensional approach using a digitized gridded terrain model. Spatial variation was addressed by treating the spatial correlation length of the velocity field as a free parameter.

Lin and Tierney (1986) predicted a mean travel time of 13,695 years for water movement through the CHnz unit with a standard deviation of 8145 years. In contrast, the mean (baseline case) travel time reported in this study was 242,261 years. The stark difference exists because Lin and Tierney's baseline case was for a recharge rate of 0.50 mm yr^{-1}, while our baseline value assumed a mean value of 0.10 mm yr^{-1}. Since 0.50 mm yr^{-1} is probably the upper limit of recharge in Yucca Mountain (Lin and Tierney 1986; Montazer et al. 1985; Sinnock et al. 1985), Lin and Tierney's (1986) estimate of mean water travel time is conservative in that it predicts much shorter travel times than are probably the case. Experience with our stochastic simulations indicates that such a high recharge rate results in fully saturated conditions in the CHnz unit, which is not consistent with field observations.

Kaplan and Yarrington (1989) performed an uncertainty analysis on travel time through the unsaturated zone at Yucca Mountain. They represented uncertainty in the input parameters with the beta probability distribution which removes subjective judgement on selection of a density function to represent the input parameter distributions. They performed Monte Carlo sampling of the input parameter distributions to generate a distribution of travel times. The range of travel times resulting from their Monte Carlo simulations covered less than an order of magnitude. The difference in the range of travel time between their analysis and the analysis presented in this report may be the result of the conceptual model and the input data assumed. They predicted travel times from the top of the Calico Hills unit into the Prow Pass Member of the Crater Flat Tuff to the water table. The model domain was represented with 11 different hydrostratigraphic units while our study assumed that the Calico Hills was a single unit. Our

assumption led to a wider distribution of the key input parameters to be sampled, which resulted in the wider distribution of travel times predicted with our model.

7.0 CONCLUSIONS

This report documents sensitivity and uncertainty analyses made to investigate the travel time distribution for water flow in the unsaturated zone at Yucca Mountain. Normalized sensitivity coefficients and Monte Carlo simulations were used to examine the response of unsaturated zone travel time to variation of five input parameters. These parameters were recharge rate, saturated hydraulic conductivity, matrix porosity, and the empirical curve-fitting parameters of the van Genuchten relations describing unsaturated moisture retention and hydraulic characteristics. The geologic unit of interest was the Calico Hills nonwelded zeolitic (CHnz) unit, one of the natural barriers to radionuclide migration from the potential Yucca Mountain high-level nuclear waste repository. A one-dimensional, single-layer model was used for steady-state simulations in this preliminary examination.

Two different analyses were conducted to investigate the sensitivity of unsaturated zone water travel time and the travel time distributions to key input parameters used in the travel time calculation. The results from these analyses demonstrated that the same parameters (recharge rate and effective porosity) are most important for estimating ground-water travel time. In the first analysis, which was based on normalized sensitivity coefficients, computed travel time was shown to be most sensitive to effective porosity. The recharge rate was the second most sensitive parameter. In the other analysis, which was based on the contribution of uncertainty or variability in input parameters to uncertainty or variability in the computed travel time, the recharge rate was found to contribute the greatest variability in the travel time distributions. The effective porosity was found to be the second most important parameter for uncertainty in the distribution of travel time. These two parameters were the same for both the single-variable and the multi-variable stochastic analyses. The remaining variables evaluated in each of the analyses were much less important than the recharge rate and effective porosity, both with respect to their contribution to sensitivity and their contribution to uncertainty.

The results of the single-variable stochastic simulations demonstrate that uncertainty in the recharge rate, saturated hydraulic conductivity, and effective porosity produce linear, or nearly linear, responses in the distribution of travel time. This occurs because these input parameters are linear multipliers in the travel time computation. The other parameters occur in the exponential equations describing the moisture retention and unsaturated hydraulic conductivity characteristics of the matrix.

The results of the single-variable stochastic simulations demonstrate that variability in recharge rate produces the greatest variability in the resulting travel time distribution. The resulting variation in travel time spans more than an order of magnitude. Variation in total porosity produces the next largest variation in travel time, nearly an order of magnitude. The van Genuchten n exponent is next, followed by saturated

hydraulic conductivity and the α that appears in the van Genuchten relationship. All of these variables contribute less than an order of magnitude variation in the resulting travel time distribution.

The results of the simultaneous multi-variable stochastic simulation demonstrate that considering all variables stochastically increases the range in travel time to approximately two orders of magnitude. A regression analysis of all the variables demonstrated that the recharge rate accounts for most of the variation of travel time, which confirms the results from the single-variable stochastic simulations.

Taken together, these results indicate that in order to reduce uncertainty in travel time estimates, important parameters to characterize are the recharge rate and the matrix porosity. Because the recharge rate has not been measured at Yucca Mountain, the uncertainty associated with this parameter is significant. Therefore, reduction of variance in unsaturated zone travel time estimates requires improved characterization of Yucca Mountain, specifically characterization of the recharge rate and the matrix porosity for the hydrostratigraphic units that comprise Yucca Mountain.

8.0 REFERENCES

10 CFR 60. 1987. U.S. Nuclear Regulatory Commission, "Disposal of high-level radioactive nuclear wastes in geologic repositories." U.S. Code of Federal Regulations.

10 CFR 960. 1987. U.S. Nuclear Regulatory Commission, "General guidelines for the recommendation of sites for nuclear waste repositories." U.S. Code of Federal Regulations.

de Marsily, Ghislain. 1986. Quantitative Hydrogeology. Academic Press, Inc. Harcourt Brace Jovanovich, Orlando, Florida.

DOE (U.S. Department of Energy). 1984. "General Guidelines for Recommendation of Sites for the Nuclear Waste Repositories: Final Siting Guidelines." 10 CFR Part 60, Federal Register, Vol. 49, p. 47714, December 6, 1984.

DOE (U.S. Department of Energy). 1986. Environmental Assessment, Yucca Mountain Site,Nevada Research and Development Area, Nevada. DOE/RW-0073, Vol. 1-9, Office of Civilian Radioactive Waste Management, Washington, D.C.

DOE (U.S. Department of Energy). 1988. Site Characterization Plan, Yucca Mountain Site, Nevada Research and Development Area, Nevada. DOE/RW-0199, Volume II, Part A, Office of Civilian Radioactive Waste Management, Washington, D.C.

Jacobson, E. A., M. D. Freshley, and F. H. Dove. 1985. Investigations of Sensitivity and Uncertainty in Some Hydrologic Models of Yucca Mountain and Vicinity. SAND84-7212, Sandia National Laboratories, Albuquerque, New Mexico.

Kaplan, P. G., and L. Yarrington. 1989. "Modeling the uncertainties in the parameter values of a layered, variably saturated column of volcanic tuff using the beta probability distribution," in: Solving Ground Water Problems with Models (proceedings of symposium sponsored by the Association of Ground Water Scientists and Engineers, February 7-9, 1989, Indianapolis, Indiana.). National Water Well Association, Worthington, Ohio. pp. 111-128.

Lin, Y. T., and M. S. Tierney. 1986. Preliminary Estimates of Groundwater Travel Time and Radionuclide Transport at the Yucca Mountain Repository Site. SAND85-2701, Sandia National Laboratories, Albuquerque, New Mexico.

Linsey, R. K., M. A. Kohler, and J. L. H. Paulhus. 1982. Hydrology for Engineers. McGraw-Hill Book Company, New York.

McCuen, R. J. 1973. "The Role of Sensitivity Analysis in Hydrologic Modeling." J. Hydrology 18:37–53.

Montazer, P., E. P. Weeks, F. Thamir, S. N. Yard, and P. B. Hofrichter. 1985. Monitoring the vadose zone in fractured tuff, Yucca Mountain, Nevada. Proceedings of the Characterization and Monitoring of the Vadose (Unsaturated) Zone Conference, Denver, Colorado, November 19-21, 1985. National Water Well Association, Worthington, Ohio. pp. 439-469.

Montazer, P., and W. E. Wilson. 1984. Conceptual Hydrologic Model of Flow in the Unsaturated Zone, Yucca Mountain, Nevada. U.S. Geological Survey Water Resources Investigation Report 84-4345, U.S. Geological Survey, Denver, Colorado.

Mualem, Y. 1976. "A New Method for Predicting the Hydraulic Conductivity of Unsaturated Porous Media." Water Resour. Res. 12(3):513-522.

Nelson, R. W. 1978. "Evaluating the Environmental Consequences of Ground-Water Contamination, 1, An Overview of Contaminant Arrival Distributions and General Evaluation Requirements." Water Resour. Res. 14(3):409-415.

Peters, R.R., and E. A. Klavetter. 1988. "A Continuum Model for Water Movement in an Unsaturated Fractured Rock Mass." Water Resour. Res. 24(3):416-430.

Peters, R. R., E. A. Klavetter, I. J. Hall, S. C. Blair, P. R. Heller, and G. W. Gee. 1984. Fracture and Matrix Hydrologic Characteristics of Tuffaceous Materials from Yucca Mountain, Nye County, Nevada. SAND84-1471, Sandia National Laboratories, Albuquerque, New Mexico.

Runchal, A. K., and B. Sagar. 1989. PORFLO-3: A Mathematical Model for Fluid Flow, Heat, and Mass Transport in Variably Saturated Geologic Media, Users Manual, Version 1.0. WHC-EP-0041, Westinghouse Hanford Company, Richland, Washington.

Sagar, B., and A. K. Runchal. 1990. PORFLO-3: A Mathematical Model for Fluid Flow, Heat, and Mass Transport in Variably Saturated Geologic Media, Theory and Numerical Methods, Volume 1. WHC-EP-0042, Westinghouse Hanford Company, Richland, Washington.

Sinnock, S., Y. T. Lin, and J. P. Brannen. 1984. Preliminary Bounds on the Expected Postclosure Performance of the Yucca Mountain Repository Site, Southern Nevada. SAND84-1492, Sandia National Laboratories, Albuquerque, New Mexico.

van Genuchten, R. 1978. Calculating the Unsaturated Hydraulic Conductivity With a New Closed-Form Analytic Model. Water Resources Program Report 78-WR-08, Department of Civil Engineering, Princeton University, Princeton, New Jersey.

van Genuchten, M. T. 1980. "A Closed Form Equation for Predicting the Hydraulic Conductivity of Unsaturated Soils." Soil Sci. Am. J. 44:982-898.

Weisburg, S. 1985. Applied Linear Regression. John Wiley and Sons, New York.

APPENDIX A

NOTATION

APPENDIX A

NOTATION

ROMAN SYMBOLS

Symbol	Concept	Dimensions
A_0	first flow coefficient (travel time algorithm)	LT^{-1}
A_1	second flow coefficient (travel time algorithm)	LT^{-1}
B	thermal buoyancy term	-
exp	exponential function (e^x)	-
F	model output variable or performance measure	-
F	F-test value (statistic)	
g	acceleration due to gravity (≈ 9.81 m s^{-2})	LT^{-2}
H	hydraulic head with respect to reference fluid density	L
i,j,k	unit vectors	-
K	hydraulic conductivity tensor	LT^{-1}
K	hydraulic conductivity with respect to subscripted direction (x,y,z)	LT^{-1}
K_S	hydraulic conductivity for saturated conditions	LT^{-1}
k	intrinsic hydraulic conductivity tensor	L^2
ln	natural logarithm (base e)	-
m	computed term in van Genuchten functional equations	-
M	fluid source/sink term (mass units)	M
M_V	fluid source/sink term (volume units)	L^3
N	number of sample observations (statistic)	-
n	van Genuchten parameter (exponential term)	-
n_E	matrix effective or flow porosity	L^3L^{-3}
n_T	matrix total porosity	L^3L^{-3}
P	pressure head	L
p	fluid pressure	$ML^{-1}T^2$
P-value	statistic indicating maximum significance level for acceptance	-
p_i	ith input parameter	-
$\overline{p_i}$	mean value of ith input parameter	-

Symbol	Concept	Dimensions
q	flow rate or recharge rate	L^3T^{-1}
R	ratio of fluid density	-
r^2	coefficient of determination (statistic)	-
S_i	sensitivity coefficient of ith parameter	-
S_{ni}	normalized sensitivity coefficient of ith parameter	-
S_S	fluid storage term	L^{-1}
T	temperature of fluid-containing geologic media	Φ
t	time	T
t^n	time n	T
U	darcian velocity in x direction	LT^{-1}
U_i	x direction darcian velocity at cell face i	LT^{-1}
U_p	pore velocity in x direction	LT^{-1}
V	Darcy velocity vector	LT^{-1}
V	darcian velocity in y direction	LT^{-1}
V^i	darcian velocity at i cell face	LT^{-1}
V_p	pore velocity in y direction	LT^{-1}
W	darcian velocity in z direction	LT^{-1}
W_p	pore velocity in z direction	LT^{-1}
X_i	x direction coordinate of cell face at index i	L
x^n	x direction coordinate at time n	L
z^*	arbitrary elevation datum	L

GREEK SYMBOLS

α	van Genuchten parameter (inverse of air entry head)	L^{-1}
α_f	compressibility of fluid	$M^{-1}LT^2$
α_s	compressibility of solid media	$M^{-1}LT^2$
β_0, β_1	regression coefficients	-
β_f	fluid compressibility	$M^{-1}LT^2$
Δ	difference	-
Δt	time step in a numerical solution	T
∂	partial derivative with respect to the subscripted variable	-
θ	volumetric moisture content	L^3L^{-3}

Symbol	Concept	Dimensions
θ^*	relative saturation	L^3L^{-3}
μ	dynamic fluid viscosity (when used in flow equations)	$L^{-1}T^{-1}$
μ	mean value of a population (when used in a statistical setting)	-
$\hat{\mu}$	mean value of a sample	-
ρ	fluid density	ML^{-3}
σ	standard deviation of a population	-
$\hat{\sigma}$	standard deviation of a sample	
σ^2	variance of a population	-
$\hat{\sigma}^2$	variance of a sample	
ρ^*	fluid density at reference temperature	ML^{-3}
ψ	soil moisture potential (= -P when P < 0)	L

SPECIAL SYMBOLS

$\vec{\nabla}$	vector differential operator ($\vec{\nabla} = i\partial_x + j\partial_y + k\partial_z$)

SUBSCRIPTS

E	effective
f	fluid
R	residual
S	saturated
s	solid
T	total
x	in x direction or at location x
y	in y direction or at location y
z	in z direction or at location z

APPENDIX B

VERIFICATION OF TRAVEL TIME COMPUTATIONAL ALGORITHM IN PORFLO-3© VERSION 1.1 AND PORMC VERSION 1.0

APPENDIX B

VERIFICATION OF TRAVEL TIME COMPUTATIONAL ALGORITHM IN PORFLO-3© VERSION 1.1 AND PORMC VERSION 1.0

Before using the PORFLO-3© version 1.1 or PORMC version 1.0 computer codes for numerical modeling and travel time computation, it was necessary to verify the accuracy and implementation of the travel time modules embedded in these codes. Though the PORFLO-3© code has been subject to independent verification testing, the travel time modules used for this study are recent untested additions to both codes. Therefore, verification was needed to ensure confidence in the numerical results. A collection of code modifications was recommended and implemented as a result of the verification testing described here. The final verification testing demonstrated that PORFLO-3© and PORMC, as corrected, provided satisfactory travel time results when compared to a semi-analytic solution.

A suitable verification problem for testing PORFLO-3© and PORMC for application to travel time studies at the Yucca Mountain Site required two specific characteristics. First, the problem needed to have an analytic solution so that results could be verified directly. Second, the problem needed to involve unsaturated flow. Jacobson et al. (1985) presented a one-dimensional, steady-state analytic solution for pressure head in the unsaturated zone along with a corresponding numerical evaluation of travel time. The following assumptions were made in deriving this solution (Jacobson et al. 1985):

- water flow is in steady-state
- the hydraulic gradient is vertically downward
- water table conditions exist at the lower boundary
- the upper boundary condition is constant flux.

The travel time solution can be referred to as a semi-analytic solution because it is a numerical evaluation, but is based on an analytic solution to obtain the flow variables.

The specific verification problem is shown schematically in Figure B.1. The problem domain is a hypothetical one-dimensional 50-m column of soil. The boundary conditions include no-flow constraints on all vertical faces (i.e., one-dimensional), a constant flux imposed on the upper boundary of 5.5×10^{-6} m d^{-1}, and a constant head imposed on the lower boundary ($\psi = 0$, i.e., the water table). The hydraulic characteristics of the soil were chosen to permit an analytic solution of the Havercamp functional relations between hydraulic head and soil moisture content and between hydraulic head and hydraulic conductivity

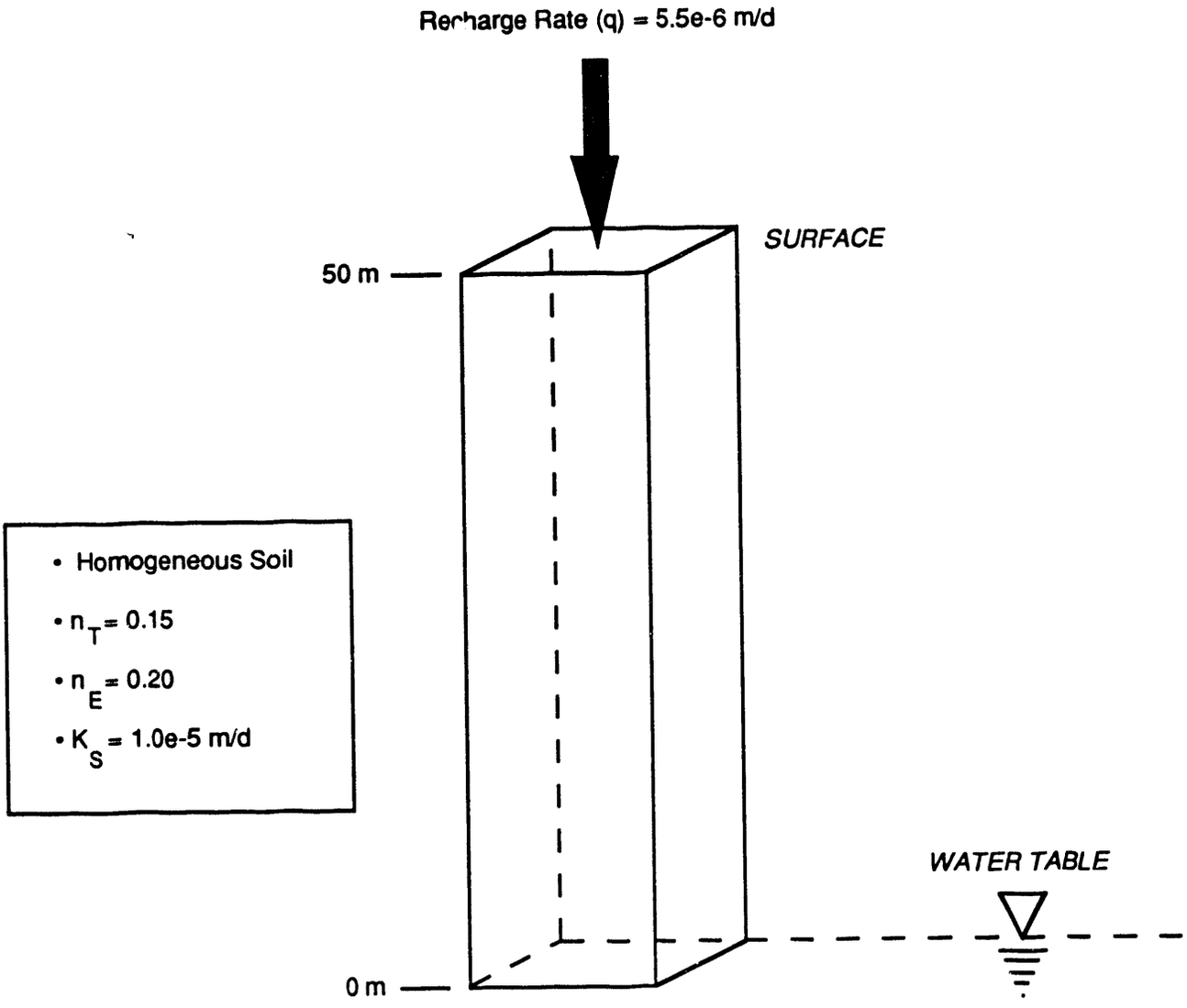

FIGURE B.1. Travel Time Algorithm Verification Problem

(Jacobson et al. 1985). The total porosity was assigned a value of 0.20 and the effective porosity a value of 0.15 (θ_R = 0.05). The saturated hydraulic conductivity was assigned a value of 1.0×10^{-5} m d^{-1}. The elevation datum was set equal to the water table, or lower boundary, for convenience.

The FORTRAN programs used by Jacobson et al. (1985) to apply the analytic solution for the flow equation and the corresponding numerical evaluation of travel time were applied to the verification problem posed here. The first program solved the flow equation and provided hydraulic head and relative saturation values at 0.5-m increments. These values were, in turn, submitted to the second program, which numerically evaluated the travel time across each 0.5-m increment and the total 50-m travel time through the problem domain.

An input file was prepared for PORFLO-3© version 1.1 to express the verification problem in identical terms. Because the Havercamp equation was not one of the unsaturated functional relations available in PORFLO-3©, the equivalent curves were computed and provided in the PORFLO-3© input in tabular form. This ensured that PORFLO-3© applied the same functional description of the soil's unsaturated characteristics as the analytic solution. A 1.0-m increment was used in the PORFLO-3© solution. The same input file was also used with PORMC. Because PORMC is essentially a stochastic version of PORFLO-3©, no difference was expected or observed in the numerical output of the two codes for this verification problem.

Iterative testing and code correction of PORFLO-3© / PORMC was required until the results were comparable to the analytic solution. Most of the problems with the travel time modules had to do with either the implementation of the algorithm within the code or with problems unique to steady-state solutions (transient solutions were the principal focus of the initial coding effort to implement the travel time modules).

The results obtained from the corrected PORFLO-3© and PORMC codes were compared with the results of the analytic solution. The values of hydraulic head and relative saturation computed by each method were equal to at least five significant figures. Figure B.2a shows the comparison of hydraulic head profiles in the 50-m soil column. Figure B.2b similarly shows the comparison of relative saturations. The semi-analytic travel time evaluation was based on these two variables, and the PORFLO-3© / PORMC algorithm is based on the velocity field across the domain. These approaches are computationally different but mathematically equivalent. The travel time results for the 50-m column are shown in Figure B.3. The semi-analytic solution gave a total travel time of 1.241×10^6 days (3,400.3 years) and the PORFLO-3© and PORMC codes gave 1.245×10^6 days (3,433.5 years). This represents a difference of 0.97% (less than 1%). Therefore, it was concluded that the PORFLO-3© and PORMC travel time algorithm (with the mentioned code modifications) was functioning properly for this class of problem and gave accurate numerical results.

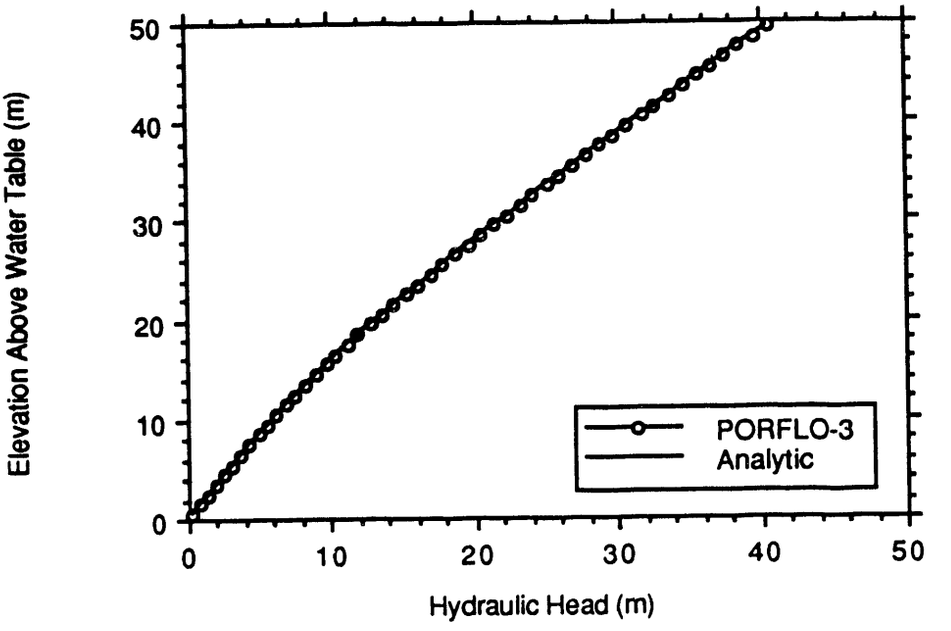

a) Hydraulic Head

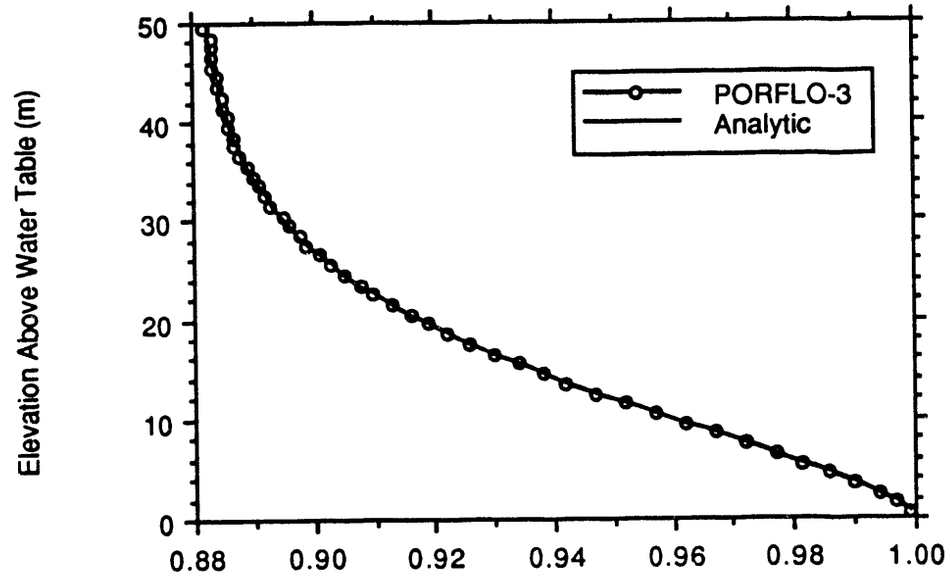

b) Saturation

FIGURE B.2. Comparison of PORMC Solution to an Analytic Solution for Verification Problem

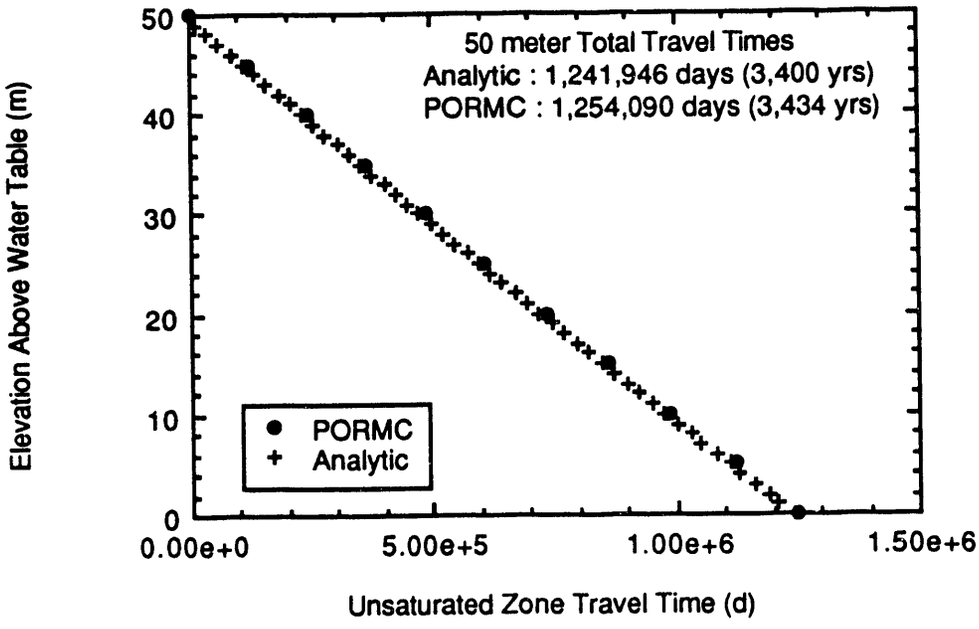

FIGURE B.3. Comparison of Unsaturated Zone Travel Time Computations

APPENDIX C

HYDROLOGIC CHARACTERISTIC DATA ON CALICO HILLS STRATIGRAPHIC UNIT

APPENDIX C

HYDROLOGIC CHARACTERISTIC DATA ON CALICO HILLS STRATIGRAPHIC UNIT

The Calico Hills nonwelded zeolitic (CHnz) unit was the subject of all simulations reported in this study. Data examined to obtain statistical descriptions of physical properties of this unit are repeated here. The stratigraphy modeled was based on that of drill hole USW-G4, though additional data were included for total matrix porosity so that a large statistical sample was available.

Because some probability distributions were assumed to follow statistical distributions involving transformations (e.g., lognormal distribution for hydraulic conductivity), transformed data are also included in the tables of this appendix. The statistics that describe these distributions are derived from transformed data rather than original data.

TABLE C.1. CHnz Bulk Density for Drill Hole USW-G4 (Peters et al. 1984)

Sample	Depth, m	Unit	Bulk Density, g m^{-3}
G4-10a	428	IV-A-z	1.39
G4-10b	428	IV-A-z	1.39
G4-10c	428	IV-A-z	1.39
G4-11a	472	IV-A-z	1.63
G4-11b	472	IV-A-z	1.61
G4-11c	472	IV-A-z	1.55
G4-4Fa	473	IV-A-z	1.51
G4-4Fb	473	IV-A-z	1.62
G4-4Fc	473	IV-A-z	1.65
G4-12a	514	IV-A-z	1.57
G4-12b	514	IV-A-z	1.57
G4-12c	514	IV-A-z	1.57
G4-13a	527	IV-B-z	1.78
G4-13b	527	IV-B-z	1.84
G4-13c	527	IV-B-z	1.83
G4-14a	529	IV-B-z	1.67
G4-14b	529	IV-B-z	1.80
G4-14c	529	IV-B-z	1.80
G4-15a	539	IV-C-z	1.77
G4-15b	539	IV-C-z	1.75
G4-15c	539	IV-C-z	1.74
G4-16a	542	IV-C-z	1.75
G4-16b	542	IV-C-z	1.69
G4-16c	542	IV-C-z	1.78
G4-5Fa	542	IV-C-z	1.67
G4-5Fb	542	IV-C-z	1.65
G4-5Fc	542	IV-C-z	1.67
G4-17a	545	IV-C-z	1.64

TABLE C.1. (contd)

Sample	Depth, m		Unit Bulk Density, g m^{-3}
G4-17b	545	IV-C-z	1.71
G4-17c	545	IV-C-z	1.63
Observations (N)			30
Mean (μ)			1.654
Standard Deviation (σ)			0.125

TABLE C.2. CHnz Unit Total Matrix Porosity Data (Lin and Tierney 1986)

Drill Hole	Depth, m	ϕ_T
UE-25a#1	403.6	0.3047
UE-25a#1	407.8	0.2749
UE-25a#1	411.2	0.2414
UE-25a#1	414.8	0.2338
UE-25a#1	425.2	0.3111
UE-25a#1	425.2	0.2864
UE-25a#1	430.1	0.3004
UE-25a#1	434.0	0.2217
UE-25a#1	440.9	0.2719
UE-25a#1	440.9	0.2615
UE-25a#1	429.7	0.2941
UE-25a#1	446.2	0.2809
UE-25a#1	450.6	0.2639
UE-25a#1	450.6	0.2632
UE-25a#1	454.2	0.2810
UE-25a#1	461.3	0.2694
UE-25a#1	462.1	0.3234
UE-25a#1	474.0	0.3211
UE-25a#1	477.5	0.2601
UE-25a#1	477.9	0.2911
UE-25a#1	489.2	0.2950
UE-25a#1	491.4	0.2345
UE-25a#1	491.4	0.1962
UE-25a#1	499.3	0.3433
UE-25a#1	500.3	0.2581
UE-25a#1	500.3	0.3074
UE-25a#1	506.6	0.3490
UE-25a#1	508.4	0.2353
UE-25a#1	508.4	0.2863
UE-25a#1	508.4	0.2800
UE-25a#1	512.2	0.3074
UE-25a#1	513.9	0.3047
UE-25a#1	515.7	0.3660

TABLE C.2. (contd)

Drill Hole	Depth, m	Dr
UE-25a#1	530.7	0.3390
UE-25a#1	545.9	0.2040
UE-25a#1	558.7	0.2058
UE-25a#1	561.4	0.3333
USW-G1	448.0	0.3651
USW-G1	458.1	0.3831
USW-G1	458.7	0.3114
USW-G1	461.7	0.3333
USW-G1	473.4	0.3522
USW-G1	478.9	0.3875
USW-G1	489.5	0.3080
USW-G1	489.5	0.3200
USW-G1	489.5	0.3036
USW-G1	489.5	0.3887
USW-G1	503.5	0.3571
USW-G1	503.5	0.3262
USW-G1	507.0	0.3347
USW-G1	508.1	0.3525
USW-G1	519.8	0.3262
USW-G1	525.0	0.3629
USW-G1	543.9	0.2366
USW-G1	558.4	0.3586
USW-G1	558.4	0.3487
USW-G1	563.0	0.3659
USW-G1	562.7	0.3534
USW-G4	436.3	0.3664
USW-G4	447.5	0.3216
USW-G4	460.7	0.3205
USW-G4	478.6	0.3593
USW-G4	496.0	0.3262
USW-G4	511.6	0.3445
USW-G4	543.9	0.2966

TABLE C.2. (contd)

Observations (N)	65
Mean ($\hat{\mu}$)	0.3063
Standard Deviation ($\hat{\sigma}$)	0.0476

TABLE C.3. CHnz Residual Moisture Saturation for Drill Hole USW-G4(Peters et al. 1984)

Drill Hole	Depth, m	θ_R
USW-G4	428.2	0.0100
USW-G4	471.8	0.1095
USW-G4	472.7	0.2017
USW-G4	513.9	0.0600
USW-G4	529.4	0.1000
USW-G4	539.2	0.2154
USW-G4	541.9	0.1330
USW-G4	541.9	0.1939
USW-G4	544.7	0.0370

Observations (N)	9
Mean ($\hat{\mu}$)	0.1178
Standard Deviation ($\hat{\sigma}$)	0.0746

TABLE C.4. CHnz Saturated Conductivity Data for Drill Hole USW-G4 (Peters et al. 1984)

Sample	Depth, m	K_S, $m\,s^{-1}$	$\ln(K_S)$, $m\,s^{-1}$	K_S, $m\,d^{-1}$	$\ln(K_S)$, $m\,d^{-1}$
G4-10	428.2	2.99×10^{-12}	-26.54	2.58×10^{-7}	-15.17
G4-11	471.8	1.31×10^{-11}	-25.06	1.13×10^{-6}	-13.69
G4-11	471.8	5.90×10^{-12}	-25.86	5.10×10^{-7}	-14.49
G4-11	471.8	1.97×10^{-11}	-24.65	1.70×10^{-6}	-13.28
G4-11	471.8	2.37×10^{-14}	-31.37	2.05×10^{-9}	-20.01
G4-4F	472.7	5.06×10^{-11}	-23.71	4.37×10^{-6}	-12.34
G4-4F	472.7	1.88×10^{-11}	-24.70	1.62×10^{-6}	-13.33
G4-4F	472.7	1.33×10^{-11}	-25.04	1.15×10^{-6}	-13.68
G4-12	513.9	4.24×10^{-12}	-26.19	3.66×10^{-7}	-14.82
G4-13	526.7	1.86×10^{-11}	-24.71	1.61×10^{-6}	-13.34
G4-13	526.7	2.45×10^{-11}	-24.43	2.12×10^{-6}	-13.07
G4-13	526.7	1.97×10^{-11}	-24.65	1.70×10^{-6}	-13.28
G4-13	526.7	4.69×10^{-14}	-30.69	4.05×10^{-9}	-19.32
G4-14	529.4	1.31×10^{-11}	-25.06	1.13×10^{-6}	-13.69
G4-14	529.4	4.59×10^{-13}	-28.41	3.97×10^{-8}	-17.04
G4-14	529.4	2.48×10^{-11}	-24.42	2.14×10^{-6}	-13.05
G4-14	529.4	1.59×10^{-12}	-27.17	1.37×10^{-7}	-15.80
G4-15	539.2	2.30×10^{-12}	-26.80	1.99×10^{-7}	-15.43
G4-16	541.9	6.47×10^{-12}	-25.76	5.59×10^{-7}	-14.40
G4-5F	541.9	6.89×10^{-12}	-25.70	5.95×10^{-7}	-14.33
G4-5F	541.9	1.83×10^{-11}	-24.72	1.58×10^{-6}	-13.36
G4-5F	541.9	2.25×10^{-11}	-24.52	1.94×10^{-6}	-13.15
G4-17	545.3	1.61×10^{-10}	-22.55	1.39×10^{-5}	-11.18
G4-17	545.3	1.97×10^{-11}	-24.65	1.70×10^{-6}	-13.28
G4-17	545.3	1.24×10^{-10}	-22.81	1.07×10^{-5}	-11.44
G4-17	545.3	1.68×10^{-12}	-27.11	1.45×10^{-7}	-15.75
Observations (N)		26			
Mean ($\hat{\mu}$)		2.29×10^{-11}	-25.66	1.97×10^{-6}	-14.30
Standard. Dev. ($\hat{\sigma}$)		3.74×10^{-11}	2.05	3.23×10^{-6}	2.05

TABLE C.5. CHnz van Genuchten Parameters for Drill Hole USW-G4 (Peters et al. 1984)

Drill Hole	α, m^{-1}	n
G4-10	2.200×10^{-2}	1.2636
G4-11	3.080×10^{-3}	1.6020
G4-4F	4.150×10^{-3}	1.8940
G4-12	6.000×10^{-3}	1.4600
G4-13	1.580×10^{-3}	1.6850
G4-14	3.700×10^{-3}	1.4960
G4-15	6.050×10^{-4}	2.4870
G4-16	4.250×10^{-3}	1.5600
G4-5F	1.200×10^{-3}	3.3220
G4-17	2.860×10^{-3}	1.6750
Observations (N)	10	10
Mean ($\hat{\mu}$)	4.943×10^{-3}	1.8445
Standard Deviation ($\hat{\sigma}$)	6.206×10^{-3}	0.6145

DISTRIBUTION

No. of Copies

OFFSITE

12 DOE Office of Scientific and Technical Information

C. P. Gertz, Associate Director
Office of Geologic Disposal, RW-20
Yucca Mountain Site Characterization Project Office
101 Convention Center Drive
Phase 2, Suite 200
Las Vegas, NV 89109

J. J. Lorenz
U.S. Department of Energy
Yucca Mountain Site Characterization Project Office, M/S 523
P.O. Box 98608
Las Vegas, NV 89193-8608

J. R. Dyer
U.S. Department of Energy
Yucca Mountain Site Characterization Project Office, M/S 523
P.O. Box 98608
Las Vegas, NV 89193-8608

R. T. Green
Center for Nuclear Waste Regulatory Analyses
6220 Culebra Road
San Antonio, TX 78228-0510

K. H. Birdsell
Los Alamos National Laboratory
Mail Stop J-665
P.O. Box 1663
Los Alamos, NM 87545

2 LATA
P.O. Box 410
Los Alamos, NM 87544
G. M. Gainer
A. Schenker

No. of Copies

4 Sandia National Laboratory
Albuquerque, NM 87185

R. W. Barnard
F. C. Lauffer
H. A. Dockery
P. G. Kaplan

ONSITE

2 DOE Field Office, Richland

D. C. Langstaff
J. J. Sutey

32 Pacific Northwest Laboratory

M. P. Bergeron	K6-77
P. G. Doctor	K6-96
R. M. Ecker	SE-UI
P. W. Eslinger	K6-96
J. W. Falco	K6-78
M. D. Freshley (2)	K6-77
J. M. Hales	K6-04
C. K. Hastings (2)	K6-96
P. C. Hays	K6-86
C. T. Kincaid	K6-77
M. R. Kreiter	K6-35
W. E. Nichols (7)	K6-77
M. L. Rockhold	K6-77
R. L. Skaggs	K6-77
J. L. Smoot	K6-77
V. R. Vermeul	K6-77
P. D. Whitney	K7-34
S. K. Wurstner	K6-77
Publishing Coordination	
Technical Report Files (5)	

END

DATE FILMED

12/06/91